

Direct test of the gauge-gravity correspondence for Matrix theory correlation functions

Masanori Hanada

*Department of Physics, University of Washington, Seattle, WA 98195-1560, USA,
E-mail: mhanada@u.washington.edu*

Jun Nishimura

*KEK Theory Center, High Energy Accelerator Research Organization (KEK),
1-1 Oho, Tsukuba, Ibaraki 305-0801, Japan, and
Department of Particle and Nuclear Physics, School of High Energy Accelerator Science,
Graduate University for Advanced Studies (SOKENDAI),
1-1 Oho, Tsukuba, Ibaraki 305-0801, Japan,
E-mail: jnishii@post.kek.jp*

Yasuhiro Sekino

*KEK Theory Center, High Energy Accelerator Research Organization (KEK),
1-1 Oho, Tsukuba, Ibaraki 305-0801, Japan,
E-mail: sekino@post.kek.jp*

Tamiaki Yoneya

School of Graduate Studies, The Open University of Japan,
2-11 Wakaba, Mihama-ku, Chiba 261-8586, Japan,
E-mail: tam@hep1.c.u-tokyo.ac.jp*

ABSTRACT: We study correlation functions in (0+1)-dimensional maximally supersymmetric $U(N)$ Yang-Mills theory, which was proposed by Banks et al. as a non-perturbative definition of 11-dimensional M-theory in the infinite-momentum frame. We perform first-principle calculations using Monte Carlo simulations, and compare the results against the predictions obtained previously based on the gauge-gravity correspondence from 10 dimensions. After providing a self-contained review on these predictions, we present clear evidence that the predictions in the large- N limit actually hold even at small N such as $N = 2$ and 3. The predicted behavior seems to continue to the far infrared regime, which goes beyond the naive range of validity of the 10D supergravity analysis. This suggests that the correlation functions also contain important information on the M-theory limit.

KEYWORDS: M(atr ix) Theories, Nonperturbative effects, Gauge-gravity correspondence.

*New address after April 1, 2010, moving from the Institute of Physics, University of Tokyo, Komaba.

Contents

1. Introduction	1
2. Matrix theory and the gauge-gravity correspondence	6
2.1 brief review of Matrix theory	6
2.2 D0-brane solution and its near-horizon limit	7
2.3 predictions for supergravity modes	9
2.4 predictions for stringy excited modes	13
3. Monte Carlo calculations on the gauge theory side	19
3.1 putting Matrix theory on a computer	19
3.2 results for supergravity modes	21
3.3 results for stringy excited modes	27
4. Summary and discussions	29
A. Spectral representation of the correlation functions	32
B. The algorithm for Monte Carlo simulation	33
C. Sign problem	36

1. Introduction

It is widely recognized nowadays that gauge theory plays an important role in understanding quantum gravity and string theory. In this context maximally supersymmetric $U(N)$ Yang-Mills theory in (0+1) dimension is of particular interest. This theory was proposed as a non-perturbative formulation of M-theory by Banks et al. (BFSS) [1] in an appropriate large- N limit. It is also called, justifiably, “Matrix theory,” the term which we will use throughout the present paper even for finite N for the sake of simplicity of nomenclature. M-theory is a conjectural 11-dimensional theory [2, 3], which was suggested to play a pivotal role in achieving a complete unification of perturbative superstring theories. When the 11th dimension of M-theory is compactified to a circle S^1 or S^1/Z_2 of radius R , the effective 10-dimensional theory one obtains at small R is assumed to be perturbative type IIA or Heterotic $E_8 \times E_8$ superstring theory, respectively, where the radius is given as $R = g_s \ell_s$ in terms of the string coupling constant g_s and the string length ℓ_s . These relations, together with the string dualities in 10 (or 9) dimensions, connect all the perturbative superstring theories. It is therefore naturally expected that deeper principles behind string theory will be revealed if one finds a concrete realization of M-theory.

The action of Matrix theory coincides with that of the effective super Yang-Mills theory describing a collection of N D0-branes [4] in type IIA superstring theory in 10 dimensions, where the Yang-Mills coupling g_{YM}^2 is proportional to the string coupling g_s . Each D0-brane with the mass $1/g_s \ell_s$ can be regarded as a Kaluza-Klein state of the 11D graviton carrying one unit of momentum along the compactified 11th direction. The proposal advocated in ref. [1] was that Matrix theory in the large- N limit with fixed g_{YM}^2 provides the exact quantum description of M-theory in spatial 9-dimensional transverse directions of the infinite momentum frame that is boosted along the circle in the 11th dimension.

Another closely related motivation for this (0+1)-dimensional theory is that it can alternatively be regarded as a regularized realization [5] of quantum (super)membrane theory in the light-cone gauge, again in the large- N limit. Supermembranes have also been regarded as basic degrees of freedom in M-theory, playing similar roles as strings in 10D superstring theory at least in some particular long-distance regime. Matrix theory can therefore be a natural basis for approaches to M-theory from the viewpoint of supermembranes, which has been quite an elusive subject for the last few decades.

From these two interpretations, the D0-branes are regarded as “partons” for both gravitons and membranes in 11 dimensions, and Matrix theory is supposed to describe the dynamics of composite systems consisting of a large number of D0-partons. Since the ’t Hooft coupling constant $\lambda = g_{\text{YM}}^2 N$ of Matrix theory must be infinitely large in the M-theory interpretation, one has to consider the strongly coupled regime of the Yang-Mills theory. Understanding the strong coupling dynamics is expected also to shed light on important problems in quantum gravity such as a microscopic description of the formation and evaporation of black holes in terms of D-branes. In spite of such prospects, it seems fair to say that no substantial progress has been made with respect to the dynamics of Matrix theory after the end of the previous century. Unfortunately, M-theory itself still remains an enigma.

Although Yang-Mills theory in (0+1) dimensions is formally super-renormalizable with respect to the UV behavior, there is very little knowledge on its strong coupling dynamics, which is essential for understanding the theory in the IR regime. A crucial obstacle is the severe IR divergence that comes from loop effects of massless fields in calculating correlation functions. While it is expected that some mass scale generated non-perturbatively makes the correlation functions finite, perturbation theory does not seem to give us useful insight on such a mechanism. In fact, by introducing mass scales through background fields, one can perform perturbative calculations, which nicely demonstrate that Matrix theory can indeed describe gravitational interactions of D0-branes in agreement with the results from supergravity. A remarkable example is the derivation of the general relativistic three-body forces [6] from the gauge theory side. This shows that the basic structure of the interaction of slowly moving D0-branes is indeed consistent with supergravity in the weakly coupled regime. However, for the purpose of studying correlation functions that would carry crucial information on the wave functions of D0-brane bound states, we cannot assume any preferred background fields.

On the other hand, the gauge-gravity correspondence has been studied intensively

over the past decade as a possible powerful approach to strongly coupled gauge theories including QCD and condensed matter systems. The best tested example is the AdS-CFT correspondence [7] between 4D $\mathcal{N} = 4$ $SU(N)$ super Yang-Mills theory (SYM) and type IIB superstring theory on the special background $AdS_5 \times S^5$. Both sides are characterized by exact (super) conformal symmetry, which greatly facilitates the analyses. From the viewpoint of string dynamics, this correspondence was motivated from the open-string/closed-string duality. In particular, if one takes the large- N limit with a large but *fixed* 't Hooft coupling λ on the SYM side, both the gravitational coupling constant $G_{10} \sim g_s^2 \ell_s^8$ and the curvature ($\sim (g_s N)^{-1/4} \ell_s^{-1}$) of the background geometry become small on the string theory side in the bulk. Therefore, one can study the gauge theory in that limit by using classical supergravity theory, which describes the low-energy limit of string theory.

In view of the general arguments based on the open-string/closed-string duality, there seems nothing that restricts the gauge-gravity correspondence to the cases with exact conformal symmetry. In particular, Matrix theory is expected to be dual to type IIA superstring theory on the background obtained in the near-horizon limit of the D0-brane solution [8]. Although neither the action of Matrix theory nor the near-horizon background of D0-branes is invariant under conformal transformations, one can transform them back to its original form by allowing the coupling constant to transform appropriately. This “generalized” conformal symmetry [9, 10] turned out to be useful in formulating the gauge-gravity correspondence at the level of operators. Unlike the familiar AdS cases, the dilaton and the curvature in the present non-conformal case are not constant in space-time in the near-horizon limit of the D0-brane solution. In fact the string coupling becomes stronger towards the origin (which corresponds to the IR region in the SYM), while the curvature becomes stronger towards the boundary (which corresponds to the UV region in the SYM). Thus there is a certain region in which we expect the supergravity description to be valid. In order for this region to extend both in the UV and IR directions, N must be sent to ∞ with a fixed but large 't Hooft coupling constant. However, the region of validity of this correspondence is slightly different from the BFSS large- N limit that is relevant to M-theory. This is not so surprising since the gauge-gravity correspondence is based on the D0-brane picture in 10-dimensional space-time, and the space-time dimension must somehow be elevated to 11 dimensions for the M-theory interpretation. Let us recall here that the dilaton carries information on the effective size of the 11th direction. Therefore, one may hope that the predictions from 10-dimensional supergravity contain important information on the 11-dimensional theory as one effectively probes the 11th direction by approaching the center of the D0-brane solution. This is one of the main issues we would like to address in the present work.

Using the gauge-gravity correspondence, two of the present authors (Y.S. and T.Y.) obtained two-point correlation functions in Matrix theory from supergravity on the D0-brane background [11]. This work was based on an extension of the general prescription proposed by Gubser, Klebanov, Polyakov and independently by Witten (GKPW) [12] for the standard AdS case, which enables us to compute correlation functions in gauge theory by evaluating the supergravity action as a functional of boundary values of the fields. Natural candidates for operators corresponding to the supergravity modes are given by

the Matrix theory currents, as suggested from a perturbative analysis with non-trivial D0-brane backgrounds [13]. They are single-trace operators with totally symmetric ordering inside the trace, which may be viewed as analogs of the BPS-operators in the $\mathcal{N} = 4$ SYM. The dictionary between these operators and the supergravity spectrum on the D0-brane background was given in ref. [11] by matching the scaling dimensions with respect to the generalized conformal symmetry.

For the operators corresponding to the massless modes, which can be described by the supergravity approximation, the two-point correlation functions are predicted to take the general form

$$\langle \mathcal{O}(t) \mathcal{O}(t') \rangle \propto \frac{1}{|t - t'|^{2\nu+1}} . \quad (1.1)$$

The supergravity approximation with the near-horizon geometry is valid in the region

$$\lambda^{-1/3} \ll |t - t'| \ll \lambda^{-1/3} N^{10/21} . \quad (1.2)$$

The exponent ν in (1.1) turned out to be fractional numbers. They are different from those determined by the canonical dimensions of the operators, but are consistent with the generalized conformal symmetry. The fact that the exponents are fractional numbers suggests that confirming this result from the gauge theory side would require a completely non-perturbative calculation of the exponents. On dimensional grounds they must be independent of the Yang-Mills coupling constant, which has a positive mass dimension. It should also be emphasized on the same grounds that the power-law behavior itself is quite non-trivial. This suggests that some mechanism for decoupling the non-perturbative dynamics from the mass scale of the Yang-Mills coupling constant is at work for this class of operators, possibly owing to supersymmetry.

From the viewpoint of the Matrix-theory conjecture, on the other hand, the power-law behavior in the IR regime is an important dynamical signature of the theory [14]. Namely, it is related to the existence of a threshold bound state (See ref. [15] and references therein.) at each finite N . This is required for consistent identification of D0-branes [4] as partons for 11-dimensional gravitons. For unprotected operators, on the other hand, it is natural to expect that two-point correlation functions are coupled with the Yang-Mills dynamics of mass generation and are given in the form of exponential functions of some dimensionless combination of the coupling constant and the coordinate distances. Indeed, such a behavior [16] has been predicted for operators corresponding to stringy excited states with large angular momentum in the plane-wave limit of the background geometry.

In the present paper, we study the two-point correlation functions by performing Monte Carlo simulation of Matrix theory. The same method [17] has been previously used to calculate the internal energy and the Wilson loop in Matrix theory at finite temperature by the authors including two of us (M.H. and J.N.) [18, 19, 20]. The results of these works are consistent with the predictions from the dual geometry in the bulk. For example, the ADM mass of the near extremal D0-brane solution gives the energy density on the gauge

theory side as a function of temperature as¹

$$\frac{1}{N^2} \frac{E}{\lambda^{1/3}} = 7.4 \left(\frac{T}{\lambda^{1/3}} \right)^{14/5}, \quad (1.3)$$

assuming that the temperature is identified with the Hawking temperature of the black hole. This relation is expected to hold under the condition $N^{-10/21} \ll T\lambda^{-1/3} \ll 1$, which coincides naturally with (1.2) under the replacement $1/T \rightarrow |t - t'|$. The Monte Carlo data on the gauge theory side not only confirms this prediction but also gives consistently the power of the sub-leading term with respect to the inverse YM coupling that are obtained from the $\alpha' (= \ell_s^2)$ corrections on the gravity (string theory) side [19]. The agreement implies that the microscopic origin of the black-hole thermodynamics has been accounted for in terms of open strings attached to the D0-branes as described by Matrix theory. These results encourage us to apply the same method to more general and subtle observables such as the correlation functions of local operators. Let us recall that the correlation functions are calculated on the gravity side [11] by extracting the response from the D0-brane background against perturbations consisting of various different components of gravitational waves propagating from the boundary towards the central region. Such observables therefore contain more detailed information on the dynamics of D0-branes than the observables that have been studied so far.

The aim of the present paper is twofold. Firstly, we give an explicit comparison of the Monte Carlo data with the predictions for supergravity states [11] and also with those for stringy excited states [16]. This provides, for the first time, a highly nontrivial test of the gauge-gravity correspondence at the level of local operators in the non-conformal case.² Secondly, we provide evidence for the possibility that the predictions obtained from the gauge-gravity correspondence actually hold beyond the naive bounds of the applicability of supergravity approximation, both with respect to the size N of the gauge group and to the range (1.2). This may be taken as an important piece of information on the behaviors of correlation functions in the M-theory regime. We hope that the present work³ would be an impetus for revisiting the Matrix theory conjecture from a new perspective.

The rest of this paper is organized as follows. In section 2, we review the gauge-gravity correspondence for Matrix theory and summarize its predictions for correlation functions. We hope that this section makes the present paper reasonably self-contained and will serve as a useful guide for the readers who are not familiar with the gauge-gravity correspondence for D0-branes and Matrix theory. In section 3, we describe our Monte Carlo method to calculate the correlation functions and compare the results with the predictions from the gauge-gravity correspondence. Section 4 is devoted to a summary and discussions.

¹The power-law behavior (1.3) is also related to the existence of the threshold bound state [21] and hence to the power-law behavior of the correlation functions. In contrast, Monte Carlo studies for the non-maximally supersymmetric cases [22] confirmed an exponential decrease at low T , which was suggested in ref. [21] by assuming the absence of the threshold bound state.

²See ref. [23] for a numerical analysis based on the discrete light-cone quantization in the $(1+1)$ -dimensional case.

³Part of the results has been reported briefly in our previous publication [24].

In appendix A, we discuss the physical meaning of the predicted two-point functions for stringy operators by considering its spectral representation. In appendix B, we explain the details of our Monte Carlo method. In appendix C, we discuss the so-called sign problem that appears in Monte Carlo studies of the present system.

2. Matrix theory and the gauge-gravity correspondence

In this section we first give a brief introduction to Matrix theory, which was proposed as a non-perturbative formulation of M-theory, and discuss the D0-brane solution in 10-dimensional supergravity, which plays a crucial role in describing the gauge-gravity correspondence in the present case. Then we review the predictions for correlation functions obtained from the gauge-gravity correspondence to the extent that would be sufficient for understanding the significance of our main results to be presented in section 3.

2.1 brief review of Matrix theory

Matrix theory is the maximally supersymmetric Yang-Mills theory in (0+1) dimensions, and it can be considered as matrix quantum mechanics. The action is given by

$$S = \int dt \operatorname{Tr} \left(\frac{1}{2g_s \ell_s} (D_t X_i)^2 + \frac{1}{4g_s \ell_s^5} [X_i, X_j]^2 + \frac{i}{2} \psi_\alpha D_t \psi_\alpha - \frac{1}{2\ell_s^2} \psi_\alpha (\gamma_i)_{\alpha\beta} [X_i, \psi_\beta] \right), \quad (2.1)$$

where the fields X_i ($i = 1, \dots, 9$) and ψ_α ($\alpha = 1, \dots, 16$) are $N \times N$ bosonic and fermionic Hermitian matrices representing the collective degrees of freedom and their superpartners associated with the D0-branes. The theory has a $U(N)$ gauge symmetry, and the covariant derivative D_t acts as $D_t = \partial_t - i[A, \cdot]$ with the gauge field A . The 16×16 gamma matrices γ_i satisfy the $SO(9)$ Clifford algebra $\{\gamma_i, \gamma_j\} = 2\delta_{ij}$. The Yang-Mills coupling g_{YM} is related to the string coupling g_s and the string length ℓ_s as $g_{\text{YM}}^2 = (2\pi)^{-2} g_s \ell_s^{-3}$. While the action (2.1) is written with the Lorentzian signature, we will use the Euclideanized time coordinate in actual calculations both on the supergravity side and on the gauge theory side.

From the viewpoint of open string theory, the above action is regarded as the low-energy effective theory for the collection of N D0-branes in type IIA superstring theory in 10 dimensions [4]. The low-energy approximation is justified in the non-relativistic limit, where $D_t X_i$ and higher derivatives are sufficiently small. The matrices X_i describe the lowest modes of open strings connecting the D0-branes, and their diagonal components represent the positions of the D0-branes in the 9-dimensional space. The $U(1)$ part, which is decoupled from the $SU(N)$ part, corresponds to the center of mass motion of the D0-branes. The $SU(N)$ part, on the other hand, represents the relative motions of the D0-branes and their interactions through open strings.

From the viewpoint of 11-dimensional M-theory, the D0-brane states represent the Kaluza-Klein modes of the graviton supermultiplet corresponding to the compactification down to 10 dimensions. The radius of the 11th direction is $R = g_s \ell_s$. The BFSS conjecture [1] is a proposal that Matrix theory in the large- N limit with fixed g_s describes exactly the dynamics of 11-dimensional gravitons in the infinite momentum frame (IMF) boosted along the 11th direction with the longitudinal momentum $P^+ = N/R$. The 9

spatial directions in the 10-dimensional interpretation now correspond to the transverse directions in the IMF. The non-relativistic approximation is justified in this frame since P^+ becomes infinitely large in the above limit. Note that the large- N limit considered by BFSS is different from the 't Hooft limit, in which $g_{\text{YM}}^2 N$ is fixed. Let us also note that the ordinary weak coupling limit with finite N and small g_s is another way to realize $P^+ \rightarrow \infty$ and hence the IMF. This alternative is usually called the “discrete light-cone quantization” (DLCQ).

The Matrix theory (2.1) is not scale invariant in the usual sense since the Yang-Mills coupling constant has a mass dimension. However, it has a generalized conformal symmetry (GCS), which can be naturally understood from the viewpoint of the D0-brane dynamics [9]. As emphasized in ref. [9], a deeper motivation for the GCS originates from the space-time uncertainty principle in string theory.⁴ Under the GCS, the coupling constant $g_{\text{YM}}^2 \propto g_s$ is scaled (with the scaling dimension 3) along with the coordinates and the fields as

$$t \rightarrow a^{-1}t, \quad X \rightarrow aX, \quad g_s \rightarrow a^3 g_s. \quad (2.2)$$

Let us recall that the string coupling $g_s = e^{\langle \phi \rangle}$ is related to the vacuum expectation value $\langle \phi \rangle$ of the dilaton in the asymptotic region. All the other generators including the special conformal transformation can also be defined, and the full conformal algebra is actually realized [9]. One can also see that the scaling transformation (2.2) corresponds to the Lorentz boost in the IMF since one can combine it with a trivial engineering rescaling ($t \rightarrow a^{-1}t, X \rightarrow a^{-1}X, \ell_s \rightarrow a^{-1}\ell_s$) to obtain the boost transformation ($t \rightarrow a^{-2}t, X \rightarrow X, R \rightarrow a^2 R$) with the 11D Planck length $\ell_P = g_s^{1/3} \ell_s$ fixed. Thus the GCS is consistent with the DLCQ interpretation of Matrix theory. To test the boost symmetry in the BFSS interpretation, on the other hand, we need to examine a much more dynamical aspect of the theory, since it is related to the scaling behavior in changing N . (See section 2.3.)

In passing we note that the Hamiltonian of this system is given as

$$H = -2P^- = R \text{Tr} \left(\frac{1}{2} \Pi^2 - \frac{1}{4g_s^2 \ell_s^6} [X_i, X_j]^2 + \dots \right), \quad (2.3)$$

where Π_i are the canonical (matrix) momenta corresponding to the matrix coordinates X_i . In the M-theory limit, $P^+ P^-$ is fixed and $P^+ \propto N$ is sent to ∞ . Thus we have to consider the spectrum of H which scales as $1/N$ near the threshold $H \sim 0$. In terms of two-point correlation functions, this amounts to considering the far IR region in which the time coordinate scales linearly in N .

2.2 D0-brane solution and its near-horizon limit

The crucial point for the gauge-gravity correspondence is that the D0-branes, which are described by the action (2.1) from the viewpoint of open strings, can also be described as a classical background in 10-dimensional supergravity from the viewpoint of closed strings.

⁴For a comprehensive discussion on the idea of the space-time uncertainty relation in string theory, see ref. [25], which also contains an extensive list of references.

The solution [26] corresponding to a stack of N D0-branes is given in the string frame as

$$\begin{aligned} ds^2 &= -h^{-1/2} dt^2 + h^{1/2} (dr^2 + r^2 d\Omega_8^2) , \\ e^\phi &= g_s h^{3/4} , \quad A_0 = -\frac{1}{g_s} (h^{-1} - 1) , \\ h &= 1 + \frac{q}{r^7} , \quad q = 60\pi^3 (g_s N) \ell_s^7 , \end{aligned} \quad (2.4)$$

where ϕ and A_0 represent the dilaton and the RR gauge field, respectively. String theory (or supergravity) on this background in the near horizon limit $h \rightarrow \frac{q}{r^7}$ is conjectured to be equivalent to Matrix theory [8, 9] under certain conditions explained below. Unlike the case of $\text{AdS}_5 \times \text{S}^5$, which corresponds to the near-horizon limit of the D3-brane solution, both the dilaton and the curvature depend on the radial coordinate. From the explicit form of the background, one can obtain the range of validity

$$(g_s N)^{1/3} N^{-4/21} \ll \frac{r}{\ell_s} \ll (g_s N)^{1/3} , \quad (2.5)$$

in which the weakly coupled supergravity description is reliable. The first inequality is necessary for the string coupling to be weak $e^\phi \ll 1$, while the second one is necessary for the curvature to be small in the string unit. Taking the near-horizon condition $\frac{r}{\ell_s} \ll (g_s N)^{1/7}$ also into account, we find that a wide range of validity can be obtained if we consider the 't Hooft limit $N \rightarrow \infty$ in the strongly coupled region, namely $g_s N \gg 1$.

Let us note here that the near-horizon limit of the D0-brane metric can be obtained by a Weyl transformation from the $\text{AdS}_2 \times \text{S}^8$ metric as

$$ds^2 = q^{2/7} h^{3/14} \left\{ \left(\frac{2}{5} \right)^2 \frac{-dt^2 + dz^2}{z^2} + \left(d\theta^2 + \cos^2 \theta d\psi^2 + \sin^2 \theta d\Omega_6^2 \right) \right\} . \quad (2.6)$$

Here the Poincaré coordinate z is related to r by

$$z = \frac{2}{5} q^{1/2} r^{-5/2} , \quad (2.7)$$

and we have chosen a special parametrization of S^8 , which will be useful in section 2.4. Given this metric (2.6), the boundary ($r \rightarrow \infty$) is formally located at $z \sim 0$. One should keep in mind, however, that the near-horizon condition $r^7 \ll q$ in the original metric (2.4) puts a natural cutoff around $z \sim q^{1/7}$.

As in the standard AdS-CFT correspondence, the time scale Δt , with which we probe the gauge theory, corresponds to the radial scale $\Delta z \sim \Delta t$ from the bulk viewpoint, since the time is common to both the bulk and boundary theories. (We will see this more explicitly in the following calculations.) This relation enables us to convert the region of validity (2.5) of the supergravity analysis into

$$\lambda^{-1/3} \ll \Delta t \ll \lambda^{-1/3} N^{10/21} \quad (2.8)$$

in terms of the time separation in the $(0+1)$ -dimensional gauge theory, where we have used

$$\lambda \equiv g_{\text{YM}}^2 N = (2\pi)^{-2} g_s N \ell_s^{-3} . \quad (2.9)$$

This region (2.8) with milder N dependence $N^{10/21}$ does not overlap on the IR side with the M-theory regime $\Delta t \sim \lambda^{-1/3} N$ mentioned below eq. (2.3). However, the Monte Carlo data presented in section 3 suggest that the supergravity results may be valid even in the IR region $\Delta t \gtrsim \lambda^{-1/3} N^{10/21}$ beyond the naive region of validity (2.8) at least for supergravity modes.

We emphasize that the whole near-horizon background including the Weyl factor, the dilaton and the RR 1-form $A_0 dt$ (up to an irrelevant constant term for the 1-form) is invariant under the same generalized scaling symmetry that appears on the gauge theory side, where we transform the parameter $g_s \rightarrow a^3 g_s$ together with the coordinates $t \rightarrow a^{-1} t$, $z \rightarrow a^{-1} z$. We can therefore classify the linearized waves in supergravity around the near-horizon background according to the transformation properties under the GCS. Although the behavior of massive fields such as stringy excited modes is qualitatively different from the massless case, we can still obtain constraints from this scaling property. See also ref. [27] for a discussion on the extension of this symmetry to the stringy level in a slightly different but related context.

2.3 predictions for supergravity modes

Let us now review the calculation of correlation functions from the supergravity side [11]. The basic idea is to apply the general prescription [12] for the gauge-gravity correspondence, which has been tested by many nontrivial examples in the standard AdS case. The prescription, formulated in the Euclideanized space-time, states that the correlation functions of Matrix theory operators $\mathcal{O}^I(t)$ can be calculated by evaluating the bulk supergravity action S_{SG} as a functional of the values of the bulk fields at the boundary as

$$e^{-S_{\text{SG}}[h]} \Big|_{h^I = h_0^I} = \left\langle e^{\sum_I \int dt h_0^I(t) \mathcal{O}^I(t)} \right\rangle. \quad (2.10)$$

The supergravity fields h^I classified by an appropriate basis $\{I\}$ are required to take a fixed value $h^I = h_0^I(t)$ at a *regulated* boundary $z = \epsilon$. In our case it is natural to assume that the boundary is located at the end of the near-horizon region $\epsilon = q^{1/7}$ (or $r = q^{1/7}$). The fields are assumed to vanish in the central region ($z \rightarrow \infty$). This condition⁵ enables us to circumvent the singularity at the center, and plays a crucial role in the following calculations. The right-hand side of (2.10) represents the generating functional for connected correlation functions of Matrix theory operators $\mathcal{O}^I(t)$, each of which couples to $h_0^I(t)$.

In ref. [11], the complete spectrum of the linearized fluctuations around the near-horizon D0-brane background was obtained. After diagonalizing the fluctuations and decomposing them into SO(9) spherical harmonics, each eigen-mode of the bosonic fluctuations is described by the (Euclidean) effective action

$$S_{\text{eff}} = \frac{q}{\kappa^2} \int dt dz z \left((\partial_0 h)^2 + (\partial_z h)^2 + \frac{\nu^2}{z^2} h^2 \right). \quad (2.11)$$

⁵From a mathematical point of view, it is needed for the kinetic operators of linear perturbations around the singular background to be self-adjoint near the center.

The field h is normalized in such a way that they are dimensionless and the action has an overall factor of $1/\kappa^2$, where $\kappa^2 \sim g_s^2 \ell_s^8$ represents the gravitational coupling. The constant ν is given by

$$\nu = \frac{2}{5}\ell + \frac{7}{5}n, \quad (2.12)$$

where ℓ is an integer which represents the SO(9) total angular momentum, and n is an integer which depends on the type of the field h ($-1 \leq n \leq 3$ for bosonic modes). In Table 1 we list the modes which we study by Monte Carlo simulation in section 3 (They are denoted in ref. [11] as v_2 , a_2 and s_3 , respectively.), and describe their properties such as the transformation property on S^8 , the value of ν , and the range of ℓ . The origin of these fields are either the graviton g_{MN} or the three-form potential C_{MNP} in 11D supergravity. The corresponding operators in Matrix theory will be specified later as (2.18)-(2.20). For a complete list of the spectrum, see ref. [11].

mode	11D origin	S^8 representation	ν	range of ℓ	operator
v_2	C_{MNP}	anti-sym. 2-form	$\frac{2}{5}\ell$	$\ell \geq 1$	J_ℓ^+
a_2	G_{MN}	vector	$\frac{2}{5}\ell$	$\ell \geq 2$	T_ℓ^+
s_3	G_{MN}	scalar	$\frac{1}{5}(2\ell - 7)$	$\ell \geq 2$	T_ℓ^{++}

Table 1: Supergravity modes and the corresponding operators in Matrix theory.

Let us compute the two-point correlation functions corresponding to the supergravity modes following the prescription in ref. [12] (in particular, the first paper). Imposing the boundary condition $h_0(t) = \int dp e^{ipt} \tilde{h}(p)$ at $z = \epsilon$, one can write the solution to the wave equation obtained from the effective action (2.11) as

$$h(t, z) = \int_{-\infty}^{\infty} dp e^{ipt} \tilde{h}(p) \frac{K_\nu(pz)}{K_\nu(p\epsilon)}, \quad (2.13)$$

where $K_\nu(pz)$ represents the modified Bessel function of the second kind, which decays exponentially as $z \rightarrow \infty$. Upon substituting the solution (2.13), the action (2.11) can be reduced to a boundary term. Setting the boundary at $z = q^{1/7}$, and expanding the action in powers of $p q^{1/7}$, we obtain

$$\begin{aligned} S &= \frac{q}{\kappa^2} \int dt \left[zh \partial_z h \right]_{z=q^{1/7}}^{z=\infty} \\ &= \frac{q}{\kappa^2} \int dp \tilde{h}(p) \tilde{h}(-p) \left[(\text{analytic in } p) + c \left(p q^{1/7} \right)^{2\nu} \left\{ 1 + \mathcal{O}\left((p q^{1/7})^2 \right) \right\} \right], \end{aligned} \quad (2.14)$$

where c is a non-zero constant factor.⁶ The terms analytic in p correspond to local divergences (delta functions and its derivatives) in the coordinate space. We ignore these terms since they do not contribute to the correlation functions at finite separations, and

⁶This factor gives the normalization of the two-point function, but we leave it as a free parameter in the following analysis. The correct normalization of some operators, such as the energy-momentum tensor, can be fixed by computing two- and three-point functions and requiring the consistency with the Ward identities. This was done in ref. [28] using an expansion in the Fefferman-Graham form. We thank K. Skenderis for discussions on this point.

furthermore we keep only the leading terms which are most relevant to the IR property of the correlation functions. From the relation (2.10), we obtain the connected part of the two-point function at large separations as

$$\langle \mathcal{O}(t) \mathcal{O}(t') \rangle = \int dp \int dp' e^{ipt} e^{ip't'} \frac{\delta}{\tilde{h}(p)} \frac{\delta}{\tilde{h}(p')} S \quad (2.15)$$

$$\sim \frac{q^{1+\frac{2}{7}\nu}}{\kappa^2} \int dp e^{ip(t-t')} p^{2\nu} \sim \frac{1}{\kappa^2} \frac{q^{1+\frac{2}{7}\nu}}{|t-t'|^{2\nu+1}}, \quad (2.16)$$

which leads to the result (1.1).

In the last step of (2.16), we have to recall that in order to have a well-defined Fourier transform $\int_{-\infty}^{\infty} dp F(p) e^{ipx}$, the L^1 integrability condition $\int_{-\infty}^{\infty} dp |F(p)| < \infty$ must be satisfied. As usual, the nonintegrability for $|p| \rightarrow \infty$ can be treated as distributions, which have appreciable supports only at short distances with respect to time separation and hence can be ignored for studying the IR behaviors. On the other hand, since our correlation functions behave as $\sim |p|^{2\nu}$ at small p , the inverse Fourier integral for the operators with $\nu < -\frac{1}{2}$ (e.g., T_2^{++} defined below) is divergent at $p \sim 0$. In these cases, we would have to invoke analytic continuation with respect to the exponent ν in defining the Fourier integral. The resulting formula is well known ($t \neq 0$),

$$\frac{1}{\sqrt{2\pi}} \int_{-\infty}^{\infty} dp |p|^{2\nu} e^{ipt} = 2^{2\nu+1/2} \frac{\Gamma(\nu+1/2)}{\Gamma(-\nu)} |t|^{-2\nu-1}. \quad (2.17)$$

Since the predictions are not trustable in the UV region, we should use this formula only for sufficiently large $|t|$.

In the above calculation the information near the boundary plays a decisive role in discriminating various operators since the boundary condition at the center is chosen such that the fields should vanish. All we need to know is the way in which the wave function is “reflected” from the central region, where the wave function (2.13) decays exponentially as $z \rightarrow \infty$. This vanishing behavior near the central strong coupling regime may be the reason why our result (2.16) can be valid in the IR region beyond the naive region of validity (2.5). On the other hand, it should also be emphasized that while these calculations are performed totally within the 10D picture, the waves reflected back to the boundary can elicit important information by sinking into the near-central region during the reflection, where the dilaton grows and hence the 11th direction begins to open up indirectly. The further we go to the IR region of the gauge theory, the longer the corresponding waves stay near the central region. Consequently the reflected waves in the IR region at the boundary can in principle store richer traces of the 11th direction than in the UV region.

Let us now describe how to find the operators in Matrix theory which correspond to the supergravity modes discussed above. For that purpose it turns out to be useful to study the currents and their moments in Matrix theory within perturbation theory around appropriate backgrounds for the matrix variables following ref. [13]. These operators are written in a single trace form, and are coupled to gravitational perturbations. One can identify them by analyzing the one-loop effective potential between diagonal blocks, which

represents gravitational interactions. The moments are constructed from the basic operators by inserting the X_i fields inside the trace and symmetrizing their ordering. Following the 11D light-cone notation in ref. [13], let us define the operators⁷

$$J_\ell^+ = \frac{1}{g_s \ell_s} C_{ij; i_1 \dots i_\ell} \text{Tr} \left(F_{ij} \tilde{X}_{i_1} \cdots \tilde{X}_{i_\ell} \right) , \quad (2.18)$$

$$T_\ell^+ = \frac{1}{g_s \ell_s} C_{i; i_1 \dots i_\ell} \text{Tr} \left((D_t X_i) \tilde{X}_{i_1} \cdots \tilde{X}_{i_\ell} \right) , \quad (2.19)$$

$$T_\ell^{++} = \frac{1}{g_s \ell_s} C_{i_1 \dots i_\ell} \text{Tr} \left(\tilde{X}_{i_1} \cdots \tilde{X}_{i_\ell} \right) , \quad (2.20)$$

where $F_{ij} = -i [X_i, X_j] / \ell_s^2$, which we will identify with the supergravity modes v_2, a_2, s_3 in Table 1, respectively. We have defined the dimensionless matrix variable $\tilde{X}_i = X_i / q^{1/7}$, which naturally corresponds to the dimensionless combination r^7 / q appearing in the D0-background in the bulk theory. We have also assumed the same global prefactor $1 / g_s \ell_s$ as in the D0-brane action (2.1) so that the engineering dimensions of these operators are now 1. It turns out that this normalization is necessary for matching the bulk modes and the gauge-theory operators with respect to the GCS.

In order for the operators to have definite $\text{SO}(9)$ angular momenta, the constant coefficients C 's must satisfy the following conditions. The coefficient $C_{i_1 \dots i_\ell}$ in (2.20) should be totally symmetric, and it should also be traceless under contraction of any two indices. The coefficient $C_{i; i_1 \dots i_\ell}$ in (2.19) should be totally symmetric, and it should also be traceless with respect to the indices $i_1 \dots i_\ell$, and anti-symmetric under the exchange of i and any of $i_1 \dots i_\ell$. The coefficient $C_{ij; i_1 \dots i_\ell}$ in (2.18) is totally symmetric, and it should also be traceless with respect to the indices $i_1 \dots i_\ell$, and anti-symmetric in i, j as well as for the exchange of i or j with any of $i_1 \dots i_\ell$.

The guiding principle in relating the gauge-theory operators with the supergravity modes is that the generalized conformal dimensions should match between the bulk fields and the gauge-theory operators. Let us define the generalized conformal dimension Δ of a gauge-theory operator $O(t)$ such as (2.18)-(2.20) by the scaling property $O(t) \rightarrow O'(t') = \rho^\Delta O(t)$ under $t \rightarrow t' = \rho^{-1} t$, $g_s \rightarrow g'_s = \rho^3 g_s$. Having in mind the calculation from the gravity side based on the effective action (2.11), we assume that the two-point functions of these operators obey the power-law behavior, and that the only length scale allowed is $q^{1/7}$ apart from the gravitational constant $g_s^2 \ell_s^8$ appearing as the overall coefficient. Then the GCS along with the usual dimensional analysis fixes the behavior of the correlation function with the above normalization to have the general form

$$\langle \mathcal{O}(t) \mathcal{O}(0) \rangle \sim \frac{1}{g_s^2 \ell_s^8} q^{(\Delta+6)/5} |t|^{-(7\Delta+12)/5} . \quad (2.21)$$

Comparing this with eq. (2.16), we get $\Delta = -1 + \frac{10}{7}\nu$. We can see from Table 1 and (2.18)-(2.20) that v_2, a_2, s_3 correspond to $J_\ell^+, T_\ell^+, T_\ell^{++}$, respectively, since the generalized

⁷The operators given in ref.[13] are of the form $J_{ij; i_1 \dots i_\ell}^{+(\ell)} = \frac{1}{g_s \ell_s} \text{Tr} (F_{ij} X_{i_1} \cdots X_{i_\ell})$. Here we have taken special combinations J_ℓ^+ , which transform irreducibly under $\text{SO}(9)$. The same remark applies to the operators T_ℓ^+ and T_ℓ^{++} as well.

conformal dimensions Δ coincide if we assign the canonical value 1 to X_i as suggested from eq. (2.2) without any anomalous dimension. (See ref. [11] for a complete dictionary between the supergravity modes and the Matrix theory currents.) Note that each of $\tilde{X}_i = X_i/q^{1/7}$ contributes $1 - \frac{3}{7} = \frac{4}{7}$ to the scaling dimension, and hence $\frac{2}{5}$ to the index ν in accord with (2.12). It is remarkable that the scaling properties can be explained with such simple assignment of dimensions with respect to the GCS. We emphasize that from a purely gauge-theoretical point of view, the appearance of the factor $q^{1/7}$ is genuinely a dynamical effect, which is difficult to understand without invoking the dual gravity theory.

As has been mentioned below eq. (2.2), the generalized scaling transformation used above is essentially equivalent to the boost transformation along the 11th direction, where the longitudinal momentum $P^+ = N/R$ is scaled by treating $1/R$ as a variable with fixed N . In the M-theory interpretation of the gauge theory, on the other hand, we fix R or g_s instead and increase N to realize the IMF. It is therefore interesting to examine the above general form from this point of view. We consider the transformation $N \rightarrow \rho N$ together with $t \rightarrow \rho t$. Then the two-point functions (2.16) scale as

$$\langle \mathcal{O}(t) \mathcal{O}(t') \rangle \sim \frac{1}{g_s^2 \ell_s^8} \frac{(g_s N \ell_s^7)^{1+\frac{2}{7}\nu}}{|t-t'|^{2\nu+1}} \rightarrow \rho^{-\frac{12\nu}{7}} \langle \mathcal{O}(t) \mathcal{O}(t') \rangle, \quad (2.22)$$

from which we obtain the weight $d_M = -6\nu/7$ for each operator under the M-theory boost. In terms of the 11D light-like coordinates, the exponent ν is expressed as

$$\nu = \frac{7}{5} (1 - n_+ + n_-) + \frac{2}{5} \ell, \quad (2.23)$$

where n_+ (n_-) is the number of upper (+) (−) light-cone indices in the operator. Thus the weight d_M is given by

$$d_M = \left(1 + \frac{1}{5}\right) (n_+ - n_- - 1) - \left(\frac{1}{7} + \frac{1}{5}\right) \ell. \quad (2.24)$$

This should be compared with the *kinematical* weight for the boost $d_M^{(\text{kin})} = (n_+ - n_- - 1) - \frac{1}{7}\ell$, where the term -1 in the parenthesis comes from the fact that the currents are supposed to be integrated over the x^- direction, and the factor of $1/7$ in front of ℓ comes from our normalization of transverse fields $\tilde{X}_i = X_i/q^{1/7}$. The weight d_M found from the gauge-gravity correspondence is indeed determined solely from the 11-dimensional index structure of the operator, but we observe interesting anomalous factors. It is therefore important to clarify whether the behavior (2.16) continues to be valid in the M-theory regime corresponding to the far IR region $|t-t'| \propto N$. Our Monte Carlo data presented in section 3.2 seem to suggest that it does. Then, it would be interesting to clarify the meaning of the anomalous behavior indicating that the transverse size is compressed by the factor of $\rho^{1/5}$ under the boost. See ref. [14] for further considerations on this issue.

2.4 predictions for stringy excited modes

In this subsection we extend the calculation of correlation functions to operators that correspond to stringy excited modes on the gravity side. We note first that this is a highly

nontrivial issue since one has to somehow generalize the GKPW prescription, which is based on the supergravity approximation. In the most general case, one would have recourse to superstring field theory for closed strings, which, however, has never been formulated successfully in non-trivial classical backgrounds even at the linearized level. This forces us to formulate the gauge-gravity correspondence in the first-quantized picture. Here we review a bulk analysis including stringy excited states [16]. The analysis treats a single string moving in the S^8 direction with J units of angular momentum with a small but finite excitation number. We can then use a semi-classical approximation for the center-of-mass motion of the string by taking the large- J limit, which is often called the plane-wave limit.

Following the well-known work in the $AdS_5 \times S^5$ case [29], we identify the string states in the plane-wave limit with the gauge-theory operators which are the counterparts of the so-called BMN operators in the $\mathcal{N} = 4$ SYM. As a typical operator, let us consider

$$\mathcal{O}_{ij,n}^J = \sum_{k=0}^J e^{2\pi i k n / J} \text{Tr} \left(X_i Z^k X_j Z^{J-k} \right), \quad (2.25)$$

with $Z = X_8 + iX_9$, where the X_8 and X_9 are taken to be the directions of classical trajectories in S^8 . The “impurities” X_i and X_j are the fields in the other transverse directions ($i, j = 1, \dots, 7$). The operator (2.25) corresponds to a state with two oscillators at the n -th level being excited. Supergravity modes discussed in the previous subsection correspond to the operators with $n = 0$. We can also consider excitation of oscillators in the t direction, which corresponds to an operator with the covariant derivative D_t inserted as an impurity.

The basis of this analysis is the prescription [30] introduced originally to solve some puzzles in the original BMN proposal. More recently, this method⁸ has been applied systematically to the evaluation of various correlation functions including three-point functions in the $AdS_5 \times S^5$ case [32, 33]. Instead of computing the energy of strings in the global AdS and identifying them with the scaling dimensions as in ref. [29], one computes the transition amplitude along a trajectory in the Euclidean AdS (with a non-trivial Weyl factor in the D0 case) connecting two points at the boundary. Note that the real trajectories in the Minkowskian AdS , in general, do *not* reach the boundary, while the tunneling trajectories in the Euclidean AdS start and end at the boundary. The amplitudes along the tunneling trajectories can then be identified with the gauge-theory correlation functions. This gives us a definite way to incorporate stringy excitations. In the present D0 case, in particular, it is crucial to use this approach since the original BMN approach would require us to consider the strings moving in a singular region near the center. That the tunneling trajectories do not reach the singularity at the center corresponds to the boundary condition in the supergravity analysis that the wave function should vanish at the center.

We now review the key steps of this approach. For simplicity, we set $\alpha' (= \ell_s^2) = 1$ throughout this subsection. Although the original analysis was given for general Dp -branes with $p < 5$, we restrict ourselves to the $p = 0$ case, which is relevant to the present work. To explain the idea in a simple setting, let us first start by considering a geodesic for an

⁸For a compact review of this approach, see ref. [31].

ordinary massive particle on the Euclidean AdS_2 , which can be obtained by minimizing the action

$$S = m \int d\tau \sqrt{\tilde{g}_{\mu\nu} \partial_\tau x^\mu \partial_\tau x^\nu} , \quad (2.26)$$

where $\tilde{g}_{\mu\nu}$ is the metric for Euclidean AdS_2 given by $ds^2 = (dt^2 + dz^2)/z^2$. If we set the mass⁹ to $m = \frac{2}{5}J$, we can regard this action (2.26) as that of a Kaluza-Klein particle with J units of angular momentum on the compactified S^8 with the time coordinate being Euclideanized. The geodesic of our interest is a half circle¹⁰

$$t = \tilde{\ell} \tanh \tau , \quad z = \frac{\tilde{\ell}}{\cosh \tau} , \quad (2.27)$$

which connects two points on the boundary separated by $|t_f - t_i| = 2\tilde{\ell}$. One finds from (2.27) that the radial cutoff ($z > \epsilon$) is related to the proper time cutoff ($|\tau| < T$) as

$$\epsilon \sim 2\tilde{\ell} e^{-T} = |t_f - t_i| e^{-T} . \quad (2.28)$$

Substituting this solution into the action (2.26), we get $S_{\text{cl}} = m \int_{-T}^T d\tau = 2mT$. The amplitude in this geodesic approximation is then proportional to

$$e^{-S_{\text{cl}}} = e^{-2mT} = \left(\frac{\epsilon}{|t_f - t_i|} \right)^{\frac{4}{5}J} . \quad (2.29)$$

This gives the large- J limit of the two-point function for the operator $\text{Tr}(Z^J)$, which is included in (2.20) as a particular case. The J dependence is indeed consistent¹¹ with the result (2.16) obtained using the wave picture for the operator T_ℓ^{++} with $\ell = J$.

In order to treat more general operators, we need to embed the above point-like classical trajectory in string theory. For that purpose we first perform a *double* Wick rotation [30] $t \rightarrow -it$, $\psi \rightarrow -i\psi$ in the D0-brane metric (2.6). One can check that the classical trajectory discussed above for the Euclideanized AdS_2 case agrees¹², in the two-dimensional subspace of time and radial coordinates, with a point-like ground-state solution for the standard (so-called ‘‘Polyakov-type’’) worldsheet action for strings around the D0-background satisfying the Virasoro conditions. The solution is independent of the worldsheet coordinate σ and is given by eq. (2.27) and $\psi = \frac{2}{5}\tau$. The period of σ is chosen to be $0 \leq \sigma \leq 2\pi\alpha$ with $\alpha = 5J/(2q^{2/7})$ so that the canonical momentum for ψ is equal to J , *i.e.*, $J = \frac{1}{2\pi} q^{2/7} \int d\sigma \dot{\psi}$. The semi-classical amplitude (2.29) can then be reproduced by evaluating the Routh function for the worldsheet string action along this solution.

⁹The factor of $2/5$ in the mass m is due to the fact that in the D0-background, the radius of S^8 is $5/2$ in units of the AdS radius. Note also that we have ignored the J -independent term in the mass m since we are dealing with the large- J limit.

¹⁰Here we take the coordinates (t, z) to be dimensionless. In order to retrieve the original coordinates, which scale like (2.2) under generalized conformal transformation, one has to multiply them by $q^{1/7}$.

¹¹The J -independent term in the exponent can be obtained by computing the zero-point energy of the superstring as described in the second paper of ref. [16], and it also agrees with the result from the GKPW prescription.

¹²The difference of the Weyl factor in the background metric can be absorbed, along the classical trajectory, by a time-dependent reparametrization of τ .

The next task is to expand the worldsheet action around this classical solution to the quadratic order in fluctuations. The quadratic terms are given as¹³

$$S^{(2)} = \frac{1}{4\pi} \int d\tau \int_0^{2\pi\alpha} d\sigma \left(\dot{x}^2 + r^{-3}(\tau) x'^2 + m_x^2 x^2 + \dot{y}_i^2 + r^{-3}(\tau) y_i'^2 + m_y^2 y_i^2 \right), \quad (2.30)$$

where $r(\tau)$ represents the trajectory in the radial direction

$$r(\tau) = \left(\frac{2 \cosh \tau}{5 \tilde{\ell}} \right)^{2/5}, \quad (2.31)$$

which is obtained from (2.27) using (2.7). The fields x and y_i ($i = 1, \dots, 7$) in (2.30) represent fluctuations within the (t, z) direction and along the S^8 direction, respectively. These fields have mass $m_x = 1$ and $m_y = 2/5$ due to the curvature around the geodesic.

The supergravity modes can be obtained by restricting ourselves to point-like configurations, which corresponds to setting $x' = y_i' = 0$ in the worldsheet action (2.30). Then the problem reduces to that of ordinary harmonic oscillators with the Hamiltonian $H = m \left(a^\dagger a + \frac{1}{2} \right)$ written schematically for each of the x and y_i oscillators. The amplitude from $\tau = -T$ to $\tau = T$ is given by

$$e^{-2HT} = e^{-2m(a^\dagger a + 1/2)T} = \left(\frac{\epsilon}{|t_f - t_i|} \right)^{2m(a^\dagger a + 1/2)}. \quad (2.32)$$

An insertion of X_i ($i = 1, \dots, 7$) into the ground state operator $\text{Tr}(Z^J)$ corresponds to exciting one of the y_i oscillators with $m = m_y$, which increases the power of $|t_f - t_i|$ in the two-point function by $2m_y = 4/5$. Similarly, an insertion of D_t corresponds to exciting the x oscillator with $m = m_x$, which increases the power by $2m_x = 2$. These rules are consistent with the results from the wave-function analysis shown in Table 1. For instance, let us consider the operator T_ℓ^{++} with $\ell = J$ and with all of the transverse directions confined in the Z -plane. Inserting D_t to it creates an operator T_ℓ^{+i} with $\ell = J - 1$. The value of ν increases by 1 as one can see from Table 1, which implies that the power increases by 2 in accord with the conclusion obtained from (2.32). Note that, in the present tunneling picture, the time direction t of gauge theory is transverse to the τ -direction near the boundary. As a consequence, we can naturally identify D_t with oscillation in a transverse direction, which supports the consistency of the present analysis. In the Minkowskian picture, this correspondence is unclear.

In order to study stringy excited modes, we need to allow x' and y_i' to be non-zero in eq. (2.30). Since the x'^2 term and the $y_i'^2$ term have τ -dependent coefficients, we have to solve the problem of quantizing oscillators with time-dependent masses. Let us explain how this can be done by taking one of the y_i oscillators as an example.¹⁴

¹³We have fixed the worldsheet metric as $\sqrt{h}h^{\tau\tau} = (\sqrt{h}h^{\sigma\sigma})^{-1} = r^{3/2}(\tau)$, as in the second paper of ref. [16]. With this choice, m_x, m_y are constant, but $x'^2, y_i'^2$ get τ dependent coefficients. If we use the conformal gauge as in the first paper of ref. [16], m_x, m_y become τ -dependent. Final results do not depend on the gauge choice.

¹⁴Impatient readers may skip these details and go directly to the final result (2.43), which is valid for states with high wave numbers.

The equation of motion for the n -th Fourier mode in σ is given by

$$\frac{d^2}{d\tau^2} y(\tau) = m^2(\tau) y(\tau) , \quad m^2(\tau) = r^{-3}(\tau) \frac{n^2}{\alpha^2} + \frac{4}{25} . \quad (2.33)$$

Let the functions $f_{\pm}(\tau)$ be the solutions to eq. (2.33) with the boundary condition $f_{\pm}(\tau) \rightarrow 0$ as $\tau \rightarrow \pm\infty$, respectively, which are normalized by $f_+ \dot{f}_- - f_- \dot{f}_+ = 1$. Let us regard $y(\tau)$ now as an operator and denote its conjugate canonical momentum by $p(\tau) = i \partial_{\tau} y(\tau)$ satisfying the canonical commutation relation $[y, p] = i$. Then we can write the solution to the time-evolution equation (2.33) as

$$y(\tau) = f_+(\tau) a + f_-(\tau) a^{\dagger} , \quad (2.34)$$

where a and a^{\dagger} are τ -independent operators satisfying $[a, a^{\dagger}] = 1$. Due to the time reflection symmetry of the problem, we have $y^{\dagger}(\tau) = y(-\tau)$, which corresponds to the reality condition in the real-time formulation, and hence $f_{\pm}(\tau) = f_{\mp}(-\tau)$ since $f_{\pm}(\tau)$ are real in our case.

Using the Hamiltonian $H(\tau) = \frac{1}{2} (p^2 + m^2(\tau) y^2)$, we can define the transition amplitude between an initial state at $\tau = -T$ and a final state at $\tau = +T$ along the tunneling trajectory. The corresponding ‘‘Euclidean’’ S-matrix is given by $S(T) = \mathcal{T} \exp \left[- \int_{-T}^T d\tau H(\tau) \right]$. Since the Hamiltonian is quadratic in a and a^{\dagger} , the S-matrix takes the form

$$S(T) = N(T) : \exp \left(\frac{1}{2} A(T) (a^{\dagger})^2 + B(T) a^{\dagger} a + \frac{1}{2} A(T) a^2 \right) : , \quad (2.35)$$

where the coefficients are expressed in terms of $f_{\pm}(T)$ as

$$A = -\frac{1}{2} \left(\frac{f_+(T)}{f_-(T)} + \frac{\dot{f}_+(T)}{\dot{f}_-(T)} \right) , \quad N^2 = 1 + B = \frac{1}{2f_-(T)\dot{f}_-(T)} . \quad (2.36)$$

We can rewrite $S(T)$ as

$$S(T) = \mathcal{N}(T) \exp \left(-\Omega b^{\dagger} b \right) , \quad (2.37)$$

where b, b^{\dagger} satisfying $[b, b^{\dagger}] = 1$ are related to a, a^{\dagger} through a T -dependent Bogoliubov transformation, and Ω is given by

$$\cosh \Omega = \frac{1}{2} \left(1 + B + \frac{1 - A^2}{1 + B} \right) . \quad (2.38)$$

In fact, with our boundary conditions for $f_{\pm}(\tau)$, it turns out that $A \sim (1 + B) \sim 0$, $b \sim a$ and $\mathcal{N} \sim (1 + B)^{1/2}$ when $T \rightarrow \infty$. Thus the final result takes the simple form

$$S(T) \sim (1 + B)^{a^{\dagger} a + 1/2} = \left(2 f_-(T) \dot{f}_-(T) \right)^{-(a^{\dagger} a + 1/2)} . \quad (2.39)$$

Let us then discuss the behavior of string excited modes. Near the boundary ($r \rightarrow \infty$), the constant term $\frac{4}{25}$ in eq. (2.33) is dominant over the time-dependent string mass term ($r^{-3}(\tau)n^2/\alpha^2$). This results from the fact that the curvature of the background in the string unit becomes strong as $r \rightarrow \infty$. However, when we study the large distance behavior

$|t_f - t_i| \rightarrow \infty$, the geodesic passes deeply through the interior region, where the string mass term dominates. In this situation it is difficult to determine the functions $f_{\pm}(\tau)$ for general excited states. We therefore restrict ourselves to excited states with higher wave numbers satisfying $n/\alpha \sim n q^{2/7}/J \gg 1$. This allows us to neglect the terms other than the string mass term, considering that the regulated boundary is placed at the end of the near horizon region ($r(\tau) \sim 1$). Therefore the equation of motion can be approximated as

$$\frac{d^2}{d\tau'^2} \tilde{y} = \frac{n^2}{\alpha^2} \tilde{y} , \quad (2.40)$$

where τ' is defined by $d\tau'/d\tau = r^{-3/2}$, and $y = r^{3/4} \tilde{y}$. The solutions to this equation are

$$f_+(\tau') = \sqrt{\frac{\alpha}{2|n|}} e^{-\frac{|n|}{\alpha} \tau'} , \quad f_-(\tau') = \sqrt{\frac{\alpha}{2|n|}} e^{\frac{|n|}{\alpha} \tau'} . \quad (2.41)$$

In terms of τ' , the boundary ($r \rightarrow \infty$) is reached at finite time T_b , which is evaluated as

$$T_b \sim \tilde{\ell} \int_{r_{\min}}^{\infty} \frac{dr}{\sqrt{\frac{25}{4} \tilde{\ell}^2 r^5 - 1}} \sim \tilde{\ell}^{3/5} . \quad (2.42)$$

Plugging this into eq. (2.39) with $T = T_b$, we obtain the S-matrix as

$$\begin{aligned} S(T) &\sim \exp \left\{ -\frac{2|n|}{\alpha} T_b \left(a^\dagger a + \frac{1}{2} \right) \right\} \\ &\sim \exp \left\{ -\hat{c}(n, J) \left(a^\dagger a + \frac{1}{2} \right) q^{1/5} |t_f - t_i|^{3/5} \right\} , \end{aligned} \quad (2.43)$$

where $\hat{c}(n, J)$ is proportional to $|n|/J$. In the last equality, we have substituted $\tilde{\ell}$ in T_b by $q^{-1/7} |t_f - t_i|$, where t_i and t_f represent the time coordinates on the boundary at both ends of the trajectory. Note that the combination $q^{1/5} |t_f - t_i|^{3/5}$ in the exponent is invariant under the generalized conformal transformation. In the case of general Dp-branes ($p < 5$), this combination takes the form $q^{1/(5-p)} |t_f - t_i|^{(3-p)/(5-p)}$.

Note that, in the conformal case $p = 3$, the power of $|t_f - t_i|$ in the exponent vanishes. Therefore, the power-law behavior of correlation functions is modified for stringy operators [32] only by the emergence of *anomalous* conformal dimensions, which depend both on the Yang-Mills coupling constant and on the wave number n . In contrast to this, for the present non-conformal case, we found the peculiar exponential behavior (2.43) in the IR region. This is an interesting prediction, which is worth being tested. We consider that the simple form $|n|/J$ of the coefficient in front of the GCS invariant combination $q^{1/5} |t_f - t_i|^{3/5}$ on the exponent may be valid only in the present limit $n/\alpha \gg 1$. In general, it could happen that the GCS invariant combination $\left(q^{1/5} |t_f - t_i|^{3/5} \right)^\eta$ appears on the exponent with some power $\eta \neq 1$. In section 3.3 we will provide some evidence that the form (2.43) is actually valid for stringy operators even with small J and n . Since the predicted behavior is quite different from the standard behavior of a massive theory, we discuss the meaning of this form based on its spectral representation in appendix A.

3. Monte Carlo calculations on the gauge theory side

In the previous section we have reviewed the calculation of two-point correlation functions in Matrix theory from the gravity side based on the gauge-gravity correspondence. In particular, the power-law behavior (2.16) was predicted for the operators (2.18)-(2.20), which correspond to the supergravity modes as summarized in Table 1. We also have a prediction (2.43) for the type of operators (2.25) corresponding to stringy excited modes in the large- J and large- n limits. In this section we calculate these two-point correlation functions directly on the gauge theory side by a Monte Carlo method. We will see that our results for $N = 2$ and $N = 3$ already show striking agreement with the predictions from the bulk side.

3.1 putting Matrix theory on a computer

We consider the Euclidean version of the action (2.1), which is given by

$$S = \frac{1}{g_{\text{YM}}^2} \int dt \text{Tr} \left(\frac{1}{2} (D_t X_i)^2 - \frac{1}{4} [X_i, X_j]^2 + \frac{1}{2} \psi_\alpha D_t \psi_\alpha - \frac{1}{2} \psi_\alpha \gamma_i^{\alpha\beta} [X_i, \psi_\beta] \right). \quad (3.1)$$

Since the coupling constant g_{YM}^2 can be absorbed by appropriate rescaling of the fields and the coordinate t , we set the 't Hooft coupling $\lambda = g_{\text{YM}}^2 N$ to unity without loss of generality. Then the strong coupling limit amounts to the IR limit.¹⁵ Since the U(1) sector of the U(N) theory is decoupled from the rest, we actually study the SU(N) theory.

In order to put the theory on a computer, we need to make the field degrees of freedom finite by introducing UV and IR cutoffs in the t -direction. The IR cutoff is introduced by compactifying the t -direction to a circle of circumference β . Since we are not interested in the thermal properties of the system in this work, we impose periodic boundary conditions on both bosons and fermions so that the supersymmetry is not broken by finite β effects. The UV cutoff is introduced by a sharp cutoff in the momentum space following the previous works [17, 18, 19, 20, 24]. This has the following advantages over the conventional lattice approach [34]. Firstly the breaking of supersymmetry is milder than in the lattice regularization, and it restores quite fast as the UV cutoff is removed [17]. Secondly one can implement the Fourier acceleration [35] without extra cost, which makes the simulation much more efficient.

When we introduce the momentum cutoff, we have to take care of the gauge symmetry. In the case of one-dimensional theory in general, one can fix the gauge completely (*i.e.*, choose a unique representative for each gauge orbit non-perturbatively) in such a way that higher momentum modes are more suppressed by the kinetic term in the action. With this gauge choice, one can also show by simple power counting that there is no UV divergence (due also to one dimension). Therefore one can retrieve gauge invariant results by sending the UV cutoff to ∞ as is checked explicitly for the bosonic theory [17].

¹⁵From the bulk point of view, once the near-horizon limit is assumed, the only spatial length scale is $\Delta X \sim (g_s N)^{1/3} \ell_s$, which corresponds on the boundary to the temporal scale $\Delta t \sim (g_s N)^{-1/3} \ell_s \sim (g_{\text{YM}}^2 N)^{-1/3}$. These estimates of ΔX and Δt are consistent with the space-time uncertainty relation $\Delta t \Delta X \gtrsim \ell_s^2$ [25].

Let us describe how we introduce the UV cutoff more in detail. First we take the static diagonal gauge $A(t) = \frac{1}{\beta} \text{diag}(\alpha_1, \dots, \alpha_N)$, where α_a can be chosen to satisfy the constraint $\max_a(\alpha_a) - \min_a(\alpha_a) < 2\pi$ by using the large gauge transformation with a non-zero winding number. We have to add to the action a Faddeev-Popov term

$$S_{\text{FP}} = - \sum_{a < b} 2 \ln \left| \sin \frac{\alpha_a - \alpha_b}{2} \right|, \quad (3.2)$$

and the integration measure for α_a is taken to be uniform. Having fixed the gauge completely by the above procedure, we can introduce a cutoff Λ in the Fourier-mode expansion

$$X_i^{ab}(t) = \sum_{n=-\Lambda}^{\Lambda} \tilde{X}_{in}^{ab} e^{i\omega n t}, \quad \psi_{\alpha}^{ab}(t) = \sum_{n=-\Lambda}^{\Lambda} \tilde{\psi}_{\alpha n}^{ab} e^{i\omega n t}, \quad (3.3)$$

where $\omega = 2\pi/\beta$, taking into account that we impose periodic boundary conditions on both $X_i^{ab}(t)$ and $\psi_{\alpha}^{ab}(t)$. Using a shorthand notation

$$\left(f^{(1)} \dots f^{(p)} \right)_n \equiv \sum_{k_1 + \dots + k_p = n} f_{k_1}^{(1)} \dots f_{k_p}^{(p)}, \quad (3.4)$$

we can write the action (3.1) as $S = S_{\text{b}} + S_{\text{f}}$, where

$$S_{\text{b}} = N\beta \left[\frac{1}{2} \sum_{n=-\Lambda}^{\Lambda} \left(n\omega - \frac{\alpha_a - \alpha_b}{\beta} \right)^2 \tilde{X}_{i,-n}^{ba} \tilde{X}_{in}^{ab} - \frac{1}{4} \text{Tr} \left([\tilde{X}_i, \tilde{X}_j]^2 \right)_0 \right], \quad (3.5)$$

$$S_{\text{f}} = \frac{1}{2} N\beta \left[\sum_{n=-\Lambda}^{\Lambda} i \left(n\omega - \frac{\alpha_a - \alpha_b}{\beta} \right) \tilde{\psi}_{\alpha,-n}^{ba} \tilde{\psi}_{\alpha n}^{ab} - (\gamma_i)_{\alpha\beta} \text{Tr} \left(\tilde{\psi}_{\alpha,-n} [\tilde{X}_i, \tilde{\psi}_{\beta}] \right)_0 \right]. \quad (3.6)$$

Integrating out the fermionic variables, one obtains the Pfaffian $\text{Pf} \mathcal{M}$, which is complex in general. (See eq. (B.19) for the definition of \mathcal{M} .) The phase of the Pfaffian turns out to be quite small for SU(2) in the parameter region investigated in the present work, but it does fluctuate for SU(3), in particular at large β . Here we simply neglect the phase and use $|\text{Pf} \mathcal{M}| = \det(\mathcal{D}^{1/4})$, where $\mathcal{D} = \mathcal{M}^{\dagger} \mathcal{M}$, instead of $\text{Pf} \mathcal{M}$. The system with finite degrees of freedom we arrive at in this way can be simulated by using the Rational Hybrid Monte Carlo (RHMC) algorithm [36], which has become quite standard nowadays in lattice QCD simulations with dynamical quarks. The details of the algorithm are given in appendix B.

An important assumption in our method is that the phase of the Pfaffian can be neglected. While the previous results [18, 19, 20, 24], which confirmed the gauge-gravity correspondence with high accuracy, certainly support this assumption, we cannot provide purely theoretical justification at the present stage. The effect of the phase can be incorporated in principle by reweighting when one calculates expectation values. This direct method becomes impractical due to huge cancellations when the phase fluctuates violently. We suspect that the fluctuation of the phase is actually smaller than that of typical extensive quantities at large β and that the phase-quenching is completely justifiable in the large- β limit. In appendix C we investigate the effect of the phase on a typical observable and show that it is indeed negligible.

3.2 results for supergravity modes

In this subsection we present our results for the two-point correlation functions of operators (2.18)-(2.20) corresponding to supergravity modes.

Let us first define the operators we study by simulating the model (3.1). The operators $J_{\ell, i_1, \dots, i_\ell}^{+ij}$ ($\ell \geq 1$) are defined by

$$J_{\ell, i_1, \dots, i_\ell}^{+ij} \equiv \frac{1}{N} \text{Str} \left(F_{ij} X_{i_1} \cdots X_{i_\ell} \right), \quad (3.7)$$

where $F_{ij} \equiv -i[X_i, X_j]$ and Str represents the symmetrized trace treating F_{ij} as a single unit. Restricting ourselves to $\ell \leq 7$, we may assume that all the indices i, j, i_1, \dots, i_ℓ are different from each other so that the traceless condition for (2.18) is trivially satisfied. The operators $T_{\ell, i_1, \dots, i_\ell}^{++}$ ($\ell \geq 2$) are defined by

$$T_{\ell, i_1, \dots, i_\ell}^{++} \equiv \frac{1}{N} \text{Str} \left(X_{i_1} \cdots X_{i_\ell} \right). \quad (3.8)$$

Restricting ourselves to $\ell \leq 9$, we may assume that all the indices i, j, i_1, \dots, i_ℓ are different from each other so that the traceless condition for (2.20) is trivially satisfied. The operator $T_{\ell, i_1, \dots, i_\ell}^{+i}$ are defined by

$$T_{\ell, i_1, \dots, i_\ell}^{+i} \equiv \frac{1}{N} \text{Str} \left((D_t X_i) X_{i_1} \cdots X_{i_\ell} \right), \quad (3.9)$$

where Str represents the symmetrized trace treating $(D_t X_i)$ as a single unit. Restricting ourselves to $\ell \leq 8$, we may assume that all the indices i, i_1, \dots, i_ℓ are different from each other so that the traceless condition for (2.19) is trivially satisfied. Due to the SO(9) symmetry, the result for the two-point correlation function for each type of operators should not depend on the assignment of the indices. Therefore we average over all possible assignment to increase the statistics in actual calculation.

Since the basic dynamical degrees of freedom in our Monte Carlo calculations are Fourier modes (3.3), the correlation functions that are directly accessible are those in the momentum space $\langle \tilde{\mathcal{O}}(p) \tilde{\mathcal{O}}(-p) \rangle$, which are related to those in the real space by the inverse Fourier transformation

$$\langle \mathcal{O}(t) \mathcal{O}(0) \rangle = \int \frac{dp}{2\pi} \langle \tilde{\mathcal{O}}(p) \tilde{\mathcal{O}}(-p) \rangle e^{ipt}. \quad (3.10)$$

Using the Fourier modes $\tilde{\mathcal{O}}_n$ defined similarly to (3.3), we can rewrite it as

$$\langle \tilde{\mathcal{O}}(p) \tilde{\mathcal{O}}(-p) \rangle = \beta \langle \tilde{\mathcal{O}}_n \tilde{\mathcal{O}}_{-n} \rangle, \quad \text{where } p = \frac{2\pi n}{\beta}. \quad (3.11)$$

Note that the factor of β on the right-hand side is needed to make the correlation function finite in the large- β limit.

The gauge-gravity correspondence predicts the two-point function in the Fourier space to behave as

$$\langle \tilde{\mathcal{O}}(p) \tilde{\mathcal{O}}(-p) \rangle \sim f(p) + g(p) |p|^{2\nu} \quad (3.12)$$

at small p as one can see from eqs. (2.14) and (2.15). Here, $f(p)$ and $g(p)$ ($g(0) \neq 0$) are analytic functions invariant under $p \leftrightarrow -p$, and hence they can be written as $f(p) = f_0 + f_2 p^2 + \dots$ and $g(p) = g_0 + g_2 p^2 + \dots$, where $g_0 \neq 0$. The coefficients are not fixed since we have focused on the most relevant term in the IR limit neglecting the overall normalization factor. Our main task is to extract the power ν by fitting the Monte Carlo data for various correlation functions to the form (3.12) and to compare it with the values predicted by the gauge-gravity correspondence.

The existence of the undetermined analytic terms in (3.12) makes the extraction of ν more difficult, in particular, for large ν . This problem can be avoided if one can make the inverse Fourier transformation (3.10) numerically. The analytic terms are transformed into local terms, and hence do not affect the power-law behavior (2.16) of correlation functions in the real space, from which one can extract the exponent ν . However, there are cases in which the inverse Fourier transformation is not possible numerically. This can happen either due to the IR behavior or due to the UV behavior. Correlation functions for operators with $\nu < -\frac{1}{2}$ (e.g., T_2^{++}) behave as $\sim |p|^{2\nu}$ at small p , and hence the inverse Fourier transform is divergent at $p \sim 0$. The correlation function for operators (e.g., T_ℓ^+) including a derivative does not fall off in the momentum space at large p , which makes the inverse Fourier transformation numerically unstable. Even in these cases, it turns out that the results we obtain directly in the momentum space are in good agreement with the prediction from the gauge-gravity correspondence.

In what follows we present our results for J_ℓ^+ , T_ℓ^{++} and T_ℓ^+ in order. In the $N = 2$ case the correlation function becomes identically zero for J_ℓ^+ (ℓ :even), T_ℓ^{++} (ℓ :odd) and T_ℓ^+ (ℓ :even) due to properties of the Pauli matrices, and hence we omit these cases.

Let us start with the correlation functions of operators J_ℓ^+ , for which the inverse Fourier transform can be calculated numerically. If we naively make the inverse transform, however, the correlation function in the real space shows oscillating behavior with the period $\delta t \sim \beta/(2\pi\Lambda)$. This is well-known as the Gibbs phenomenon, and it is an artifact of the sharp cutoff in the momentum space. In the present case, we may naturally expect

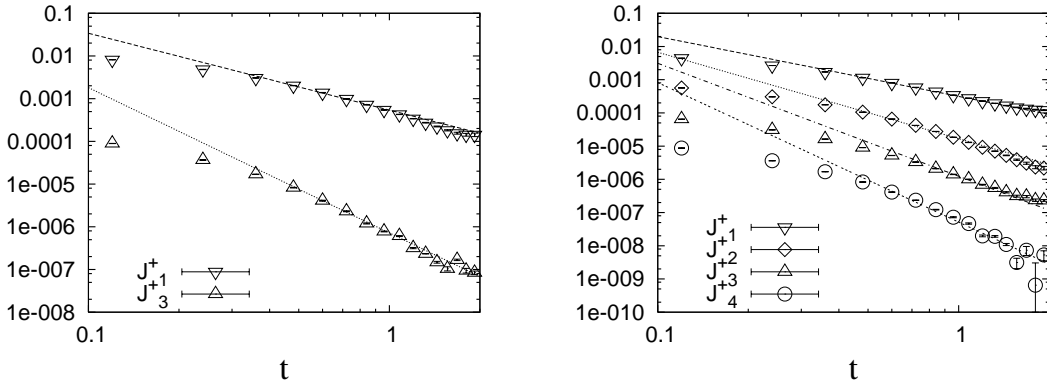


Figure 1: The log-log plot of the correlator $\langle J_\ell^+(t) J_\ell^+(0) \rangle$ with $\ell = 1, 3$ for $N = 2$ (Left) and with $\ell = 1, 2, 3, 4$ for $N = 3$ (Right). The cutoff parameters are chosen as $\beta = 4$ and $\Lambda = 16$. The straight lines represent the power-law behavior predicted by the gauge-gravity correspondence.

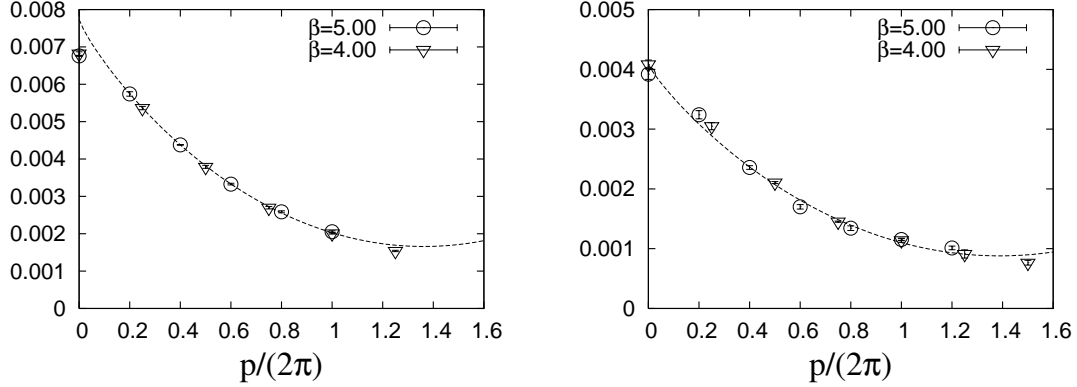


Figure 2: The correlator $\langle \tilde{J}_1^+(p) \tilde{J}_1^+(-p) \rangle$ is plotted as a function of p for $N = 2$ (Left) and $N = 3$ (Right). The extrapolation to $\Lambda = \infty$ is made at each p . The dashed line represents a fit to the behavior (3.15), from which we obtain $\nu = 0.42(6)$ for $N = 2$ and $\nu = 0.43(5)$ for $N = 3$. The predicted value is $\nu = 2/5$.

that the large- p behavior of the two-point correlation functions is given by

$$\langle \tilde{J}_\ell^+(p) \tilde{J}_\ell^+(-p) \rangle \sim \frac{\kappa}{p^2} . \quad (3.13)$$

Indeed our data can be nicely fitted to this behavior at large p , and we can obtain the coefficient κ reliably. The correlation function in the real space can then be obtained as

$$\langle J_\ell^+(t) J_\ell^+(0) \rangle = \langle \tilde{J}_{\ell 0}^+ \tilde{J}_{\ell 0}^+ \rangle + \sum_{n>0} 2 \cos\left(\frac{2\pi n t}{\beta}\right) \langle \tilde{J}_{\ell n}^+ \tilde{J}_{\ell, -n}^+ \rangle , \quad (3.14)$$

where we extend the sum over n beyond Λ using the form (3.13) up to $n = 1000$. The results obtained in this way are shown in fig. 1 for $N = 2$ (Left) and $N = 3$ (Right). The cutoff parameters are $\beta = 4$ and $\Lambda = 16$. We fit our data points for $n = 10, 11$ and 12 to (3.13), and use the form for $12 < n \leq 1000$ in the sum (3.14). Straight lines represent the power-law behavior $\text{const.}/t^{2\nu+1}$ with $\nu = 2\ell/5$, which is predicted for $N = \infty$ from the gauge-gravity correspondence. In the large- t region ($t \gtrsim 0.5$), the power law is reproduced with remarkable precision up to the IR cutoff scale ($t \lesssim \beta/2$). Moreover, the results for $N = 2$, which are obtained only for odd ℓ for the reason mentioned above, already show the power-law behavior with the same exponent as predicted by the supergravity analysis. This suggests that the exponents are actually independent of $N(\geq 2)$.

The consistency with the gauge-gravity correspondence can also be seen directly in the momentum space. Since we are interested in the IR behavior, let us restrict ourselves to the behavior at small p . According to the gauge-gravity correspondence, the first few terms relevant at small p for $\ell = 1, 2, 3, 4$ are

$$\langle \tilde{J}_\ell^+(p) \tilde{J}_\ell^+(-p) \rangle \simeq \begin{cases} a + b|p|^{2\nu} + c p^2 & \text{for } \ell = 1, 2 , \\ a + b p^2 + c |p|^{2\nu} & \text{for } \ell = 3, 4 , \end{cases} \quad (3.15)$$

where $\nu = 2\ell/5$. In fig. 2 we show our results for J_1^+ with $N = 2$ (Left) and $N = 3$ (Right). At each p we made an extrapolation to $\Lambda = \infty$ assuming that the finite Λ effect is of the

	a	b	c	ν	ν_{pred}
J_1^+	$0.40(1) \times 10^{-2}$	$-0.8(1) \times 10^{-3}$	$0.32(8) \times 10^{-4}$	$0.43(5)$	0.4
J_2^+	$0.438(1) \times 10^{-3}$	$-0.58(7) \times 10^{-4}$	$0.26(9) \times 10^{-4}$	$0.84(3)$	0.8
J_3^+	0.47×10^{-4}	-0.38×10^{-5}	0.17×10^{-5}	1.18	1.2
J_4^+	$0.582(6) \times 10^{-5}$	$-0.12(5) \times 10^{-6}$	$0.57(4) \times 10^{-8}$	*	1.6

Table 2: The parameters obtained by fitting our results for the correlators $\langle \tilde{J}_\ell^+(p) \tilde{J}_\ell^+(-p) \rangle$ with $N = 3$ to the behavior (3.15). The values of ν predicted from the gauge-gravity correspondence are shown on the right most column. For J_3^+ , the fitting errors are not shown since we can use only 4 data points for the fit. For J_4^+ , we present the values of a , b and c obtained by fixing ν to the predicted value 1.6 since the fitting errors turned out to be large otherwise.

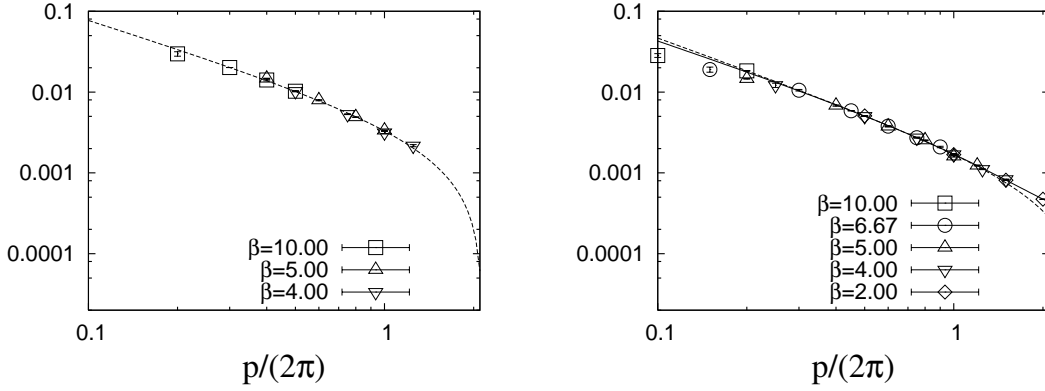


Figure 3: The log-log plot of the correlator $\langle \tilde{T}_2^{++}(p) \tilde{T}_2^{++}(-p) \rangle$ for $N = 2$ (Left) and $N = 3$ (Right). The extrapolation to $\Lambda = \infty$ is made at each p . The dashed line is a fit to the behavior (3.16), from which we obtain $\nu = -0.57(3)$ and $\nu = -0.66(2)$ for $N = 2$ and $N = 3$, respectively. For the $N = 3$ case, we can fit the data up to $p/(2\pi) = 2$ as shown by the solid line by including a higher order term $d|p|^{2\nu+2}$ in (3.16), which gives $\nu = -0.61(2)$. The predicted value is $\nu = -3/5$.

order of $O(1/\Lambda)$.¹⁶ By fitting our results at $0 < p/(2\pi) \leq 1$ to the behavior (3.15), we obtain $\nu = 0.42(6)$ and $\nu = 0.43(5)$ for $N = 2, 3$, respectively, which are consistent with the predicted value $\nu = 2/5$. The same analysis can be performed also for J_ℓ^+ with $\ell = 2, 3, 4$. The values of the parameters obtained by fitting our data for $N = 3$ are summarized in Table 2. The fits are reasonable, and they are consistent with the predictions from the gauge-gravity correspondence.

Let us next consider the operator T_ℓ^{++} for $\ell = 2, 3, 4, 5$. The gauge-gravity correspondence predicts $\nu = (2\ell - 7)/5$ [11]. The $\ell = 2, 3$ cases are of particular interest since the supergravity analysis predicts $\nu = -3/5$ and $\nu = -1/5$, respectively, which are negative. From (3.12), the correlation function in the momentum space is expected to behave as

$$\langle \tilde{T}_\ell^{++}(p) \tilde{T}_\ell^{++}(-p) \rangle = a|p|^{2\nu} + b \quad \text{for } \ell = 2, 3 \quad (3.16)$$

¹⁶In most cases we used the data for $\Lambda = 8, 12, 16$. In the $N = 3$ case with $p/(2\pi) \leq 3/\beta$ for $\beta \geq 5$, we had to use the data for $\Lambda = 6, 8, 12$ since the data for $\Lambda = 16$ had too large statistical errors. The extrapolation to $\Lambda = \infty$ seems to be fine, though, since finite Λ effects are less severe in the small p region.

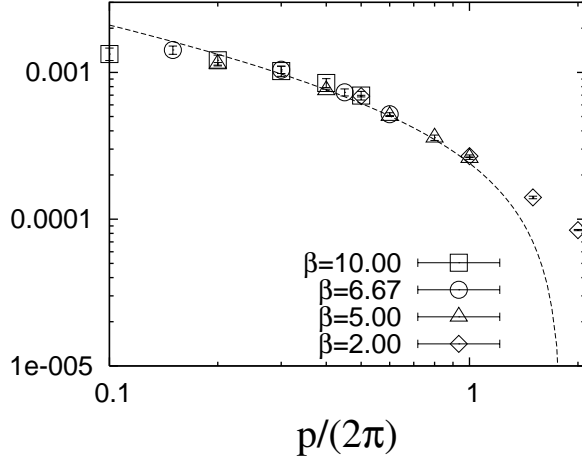


Figure 4: The log-log plot of the correlator $\langle \tilde{T}_3^{++}(p) \tilde{T}_3^{++}(-p) \rangle$ for $N = 3$. The extrapolation to $\Lambda = \infty$ is made at each p . The dashed line represents a fit to the behavior (3.16) within the range is $2/\beta \leq p/(2\pi) \leq 0.8$, which gives $\nu = -0.2(1)$. The predicted value is $\nu = -1/5$.

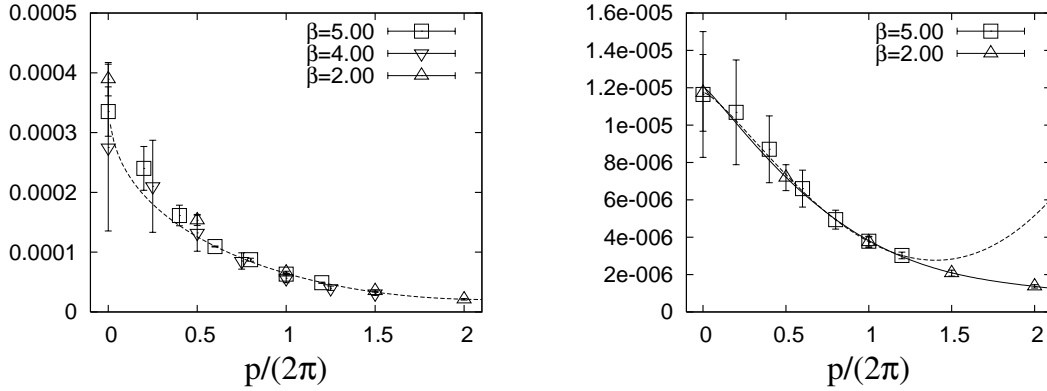


Figure 5: (Left) The correlator $\langle \tilde{T}_\ell^{++}(p) \tilde{T}_\ell^{++}(-p) \rangle$ is plotted as a function of p for $\ell = 4$ (Left) and $\ell = 5$ (Right) in the $N = 3$ case. The extrapolation to $\Lambda = \infty$ is made at each p . The dashed line represents a fit to the behavior (3.17), which gives $\nu = 0.19(3)$ and $\nu = 0.7(1)$ for $\ell = 4$ and $\ell = 5$, respectively. For the $\ell = 5$ case, we can fit the data up to $p/(2\pi) = 2$ as shown by the solid line by including a higher order term $d|p|^{2\nu+2}$ in (3.17), which gives $\nu = 0.60(9)$. The predicted values are $\nu = 1/5$ and $\nu = 3/5$ for $\ell = 4$ and $\ell = 5$, respectively.

at small p . Note that the leading term is divergent in the IR limit $p \rightarrow 0$ unlike the previous cases. In particular, the inverse Fourier transform (3.10) is ill-defined for $\ell = 2$. This is somewhat reminiscent of the free-field behavior $\sim 1/p^2$ albeit with a milder form. In fig. 3 we show a log-log plot in the case of $\ell = 2$ for $N = 2$ (Left) and $N = 3$ (Right). For the $N = 2$ case, we can fit all the data in the figure with $p/(2\pi) \geq 1/\beta$ to (3.16), which gives $\nu = -0.57(3)$. For the $N = 3$ case, we can fit the data within $1/\beta < p/(2\pi) \leq 1$ as represented by the dashed line, which gives $\nu = -0.66(2)$. By including a higher order term $d|p|^{2\nu+2}$ in (3.16), however, we can fit all the data in the figure with $p/(2\pi) \geq 1/\beta$ as represented by the solid line, which gives $\nu = -0.61(2)$. These results are consistent

	a	b	c	ν	ν_{pred}
T_2^{++}	$0.249(6) \times 10^{-1}$	$-0.13(2) \times 10^{-2}$	*	$-0.61(2)$	-0.6
T_3^{++}	$0.23(5) \times 10^{-2}$	$-0.8(6) \times 10^{-3}$	*	$-0.2(1)$	-0.2
T_4^{++}	$0.38(3) \times 10^{-3}$	$-0.16(3) \times 10^{-3}$	$0.45(7) \times 10^{-6}$	$0.19(3)$	0.2
T_5^{++}	$0.12(5) \times 10^{-4}$	$-0.17(3) \times 10^{-5}$	$0.2(1) \times 10^{-6}$	$0.60(9)$	0.6

Table 3: The parameters obtained by fitting our results for the correlators $\langle \tilde{T}_\ell^{++}(p) \tilde{T}_\ell^{++}(-p) \rangle$ with $N = 3$ to (3.16) for $\ell = 2, 3$ and to (3.17) for $\ell = 4, 5$. The values of ν predicted from the gauge-gravity correspondence are shown on the right most column. For $\ell = 2$ and 5, we also include a term $d|p|^{2\nu+2}$ with the coefficient $d = 0.95(6) \times 10^{-4}$ and $d = -0.24(7) \times 10^{-8}$, respectively.

with the predicted value $\nu = -3/5$. The deviation from the behavior (3.16) at smaller p around the IR bound ($\sim \beta^{-1}$) is naturally interpreted as finite β effects. In fig. 4 we plot the result for T_3^{++} in the $N = 3$ case. Fitting our data to the behavior (3.16), we obtain $\nu = -0.2(1)$, which is consistent with the predicted value $\nu = -1/5$.

In the $\ell = 4, 5$ cases, the gauge-gravity correspondence predicts

$$\langle \tilde{T}_\ell^{++}(p) \tilde{T}_\ell^{++}(-p) \rangle = a + b|p|^{2\nu} + cp^2 \quad (3.17)$$

at small p , where $\nu = 1/5, 3/5$ for $\ell = 4, 5$, respectively. In fig. 5 we plot the correlation functions for T_4^{++} (Left) and T_5^{++} (Right) with $N = 3$. The data at small p have large statistical errors. We consider this as a consequence of the fact that the operators T_ℓ^{++} with large ℓ are composed of large powers of X without derivatives or commutators, and hence they are more affected by the large fluctuations of the low-momentum modes of the X field. For the $N = 2$ case, we can fit all the data in the figure to (3.17), which gives $\nu = 0.19(3)$. For the $N = 3$ case, we can fit the data with $p/(2\pi) \leq 1.2$ as represented by the dashed line, which gives $\nu = 0.7(1)$. By including a higher order term $d|p|^{2\nu+2}$ in (3.17), however, we can fit all the data in the figure as represented by the solid line, which gives $\nu = 0.60(9)$. These results are consistent with the predicted values $\nu = 1/5, 3/5$ for $\ell = 4, 5$, respectively. In Table 3 we present the values of the fitting parameters obtained for T_ℓ^{++} ($\ell = 2, 3, 4, 5$) in the $N = 3$ case.

As the last example of operators corresponding to supergravity modes, let us consider the operator T_ℓ^+ defined by (3.9). The peculiarity of this operator is that it involves a derivative with respect to t . As a result, the corresponding two-point correlation functions do not decrease as $\sim 1/p^2$ unlike the previous examples. Although finite Λ effects turned out to be rather large, we were able to extrapolate our results obtained at $\Lambda = 6, 8, 12, 16$ to $\Lambda = \infty$. In fig. 6 we plot $\langle \tilde{T}_2^+(p) \tilde{T}_2^+(-p) \rangle$ for $N = 3$, $\beta = 5$. Fitting the data in the region $0 \leq p/(2\pi) < 1$ to the behavior

$$\langle \tilde{T}_2^+(p) \tilde{T}_2^+(-p) \rangle = a + b|p|^{2\nu} + cp^2, \quad (3.18)$$

we obtain $\nu = 0.80(3)$, which is consistent with the predicted value $\nu = 4/5$.

Finally, let us briefly comment on the sign of the leading term in all the correlation functions studied in this paper. Our data together with the formula (2.17) shows that the

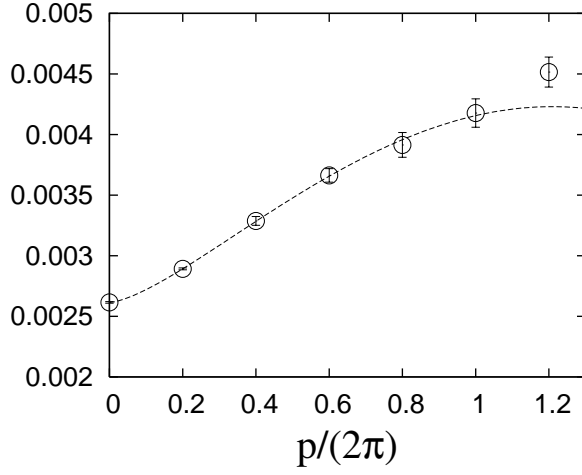


Figure 6: The correlator $\langle \tilde{T}_2^+(p) \tilde{T}_2^+(-p) \rangle$ is plotted for $N = 3$ and $\beta = 5$. The extrapolation to $\Lambda = \infty$ is made at each p . The dashed line represents a fit to the behavior (3.18) with $a = 2.614(2) \times 10^{-3}$, $b = 3.1(3) \times 10^{-4}$, $c = -1.1(3) \times 10^{-4}$, and $\nu = 0.80(3)$. The value of ν predicted from the gauge-gravity correspondence is $\nu = 4/5$.

correlation functions obey the positive IR behavior in the real space suggested from the (reflection) positivity, except for the operators T_ℓ^{++}, T_ℓ^+ with $\ell = 2$. In the case of T_2^{++} , we note that the naive L^1 integrability condition for the inverse Fourier transformation is violated in the IR region since $\langle \tilde{T}_2^{++}(p) \tilde{T}_2^{++}(-p) \rangle \sim |p|^{-6/5}$ at $p \rightarrow 0$. The non-positivity may be attributed to this property in analogy with the apparent violation of positivity that occurs for the free-field propagator $\langle X(t)X(0) \rangle = -|t|/2 + \text{const.}$, which is related with the divergent momentum-space behavior $1/p^2$ at $p = 0$. In the case of T_2^+ , the momentum-space correlation function does not decrease for $p \rightarrow \infty$ as exhibited in fig. 6, and hence the UV behavior does not satisfy the L^1 integrability, either. Note, however, that the non-integrability at the UV region does not directly affect the leading IR behavior. Therefore the situation is rather unclear.

3.3 results for stringy excited modes

In this subsection we present our Monte Carlo results for operators corresponding to stringy excited modes. Let us first consider the BMN-type operator (2.25). The result (2.43) based the gauge-gravity correspondence suggests that the corresponding two-point functions behave as

$$\langle \mathcal{O}_{ij,n}^J(t) \mathcal{O}_{ij,n}^{J\dagger}(0) \rangle \sim a \exp(-b t^{3/5}) , \quad (3.19)$$

up to a power behaved correction factor. This prediction was obtained in the plane-wave limit, which is justified when the angular momentum J and the wave number n are both large.

In what follows we calculate the correlation function on the gauge theory side and compare the results with the prediction (3.19). For that purpose we make an inverse Fourier transformation as we did for the operator J_ℓ^+ in the previous section. In order to

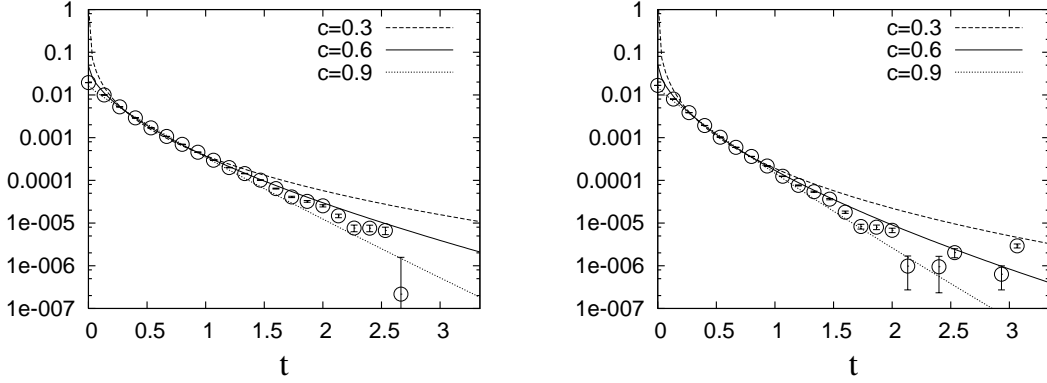


Figure 7: The two-point correlation function of the BMN-type operator (2.25) is plotted in the real space for $J = 2$ (Left) and $J = 3$ (Right) with $n = 1$. The matrix size is $N = 3$ and the cutoff parameters are $1/\beta = 0.15$ and $\Lambda = 16$. The curves represent the fits to the form $a \exp(-bt^c)$ with $c = 0.3, 0.6, 0.9$. Fitting the data in $0.2 \leq t \leq 1.5$, we obtain $c = 0.63(1)$ and $c = 0.66(2)$ for $J = 2$ and $J = 3$, respectively.

avoid the Gibbs phenomenon associated with the sharp UV cutoff, we extrapolate our data to larger momenta assuming the form $\frac{\kappa}{p^2 + m^2}$. We take the UV cutoff to be $\Lambda = 16$, and determine the parameters κ and m^2 by fitting the data at $p = 2\pi k/\beta$ for $k = 8, \dots, 12$. Similarly to the case of T_ℓ^{++} with $\ell = 4, 5$ shown in fig. 5, the two-point functions of the BMN-type operators for $J \geq 4$ have large statistical errors in the small p region, which propagates to the real-space correlator through the inverse Fourier transformation. Therefore, we restrict ourselves to $J = 2, 3$.

Figure 7 shows the results for BMN-type operators with $J = 2$ and $J = 3$, respectively. The wave number n in the operator (2.25) is set to $n = 1$. Fitting the data within $0.2 \leq t \leq 1.5$ to the form $a \exp(-bt^c)$, we obtain $c = 0.63(1)$ and $c = 0.66(2)$ for $J = 2$ and $J = 3$, respectively, which are close to the value $3/5$ predicted for large J and n . The deviations observed at large t ($\gtrsim 2$) can be attributed to finite- β effects. The coefficient b is predicted to be proportional to n/J for large n and J with $n \gg J$. The values of b obtained from the fit by fixing c to be $3/5$ are $b = 4.70$ and $b = 5.40$ for $J = 2$ and $J = 3$, respectively. This suggests that the coefficient b has more nontrivial dependence than $b \propto n/J$ for small n and J .

Next we consider a non-BPS type operator of the form

$$\mathcal{O}_{kl} \equiv \text{Tr} \left(F_{kl} \sum_{i=1}^9 (X_i)^2 \right), \quad (3.20)$$

where $F_{kl} = -i[X_k, X_l]$. Note that this operator does not belong to the type of operators J_ℓ^+ in (2.18) since the traceless condition is not satisfied. In fig. 8 we show our results for the two-point correlation function $\langle \mathcal{O}_{kl}(t) \mathcal{O}_{kl}^\dagger(0) \rangle$, which look surprisingly similar to the results for the BMN-type operators. The log-log plot shown on the right reveals clear deviation from a straight line behavior corresponding to the power law. Fitting the data in the region $0.2 \leq t \leq 1.5$ to the form $a \exp(-bt^c)$, we obtain $c = 0.58(2)$, which is consistent

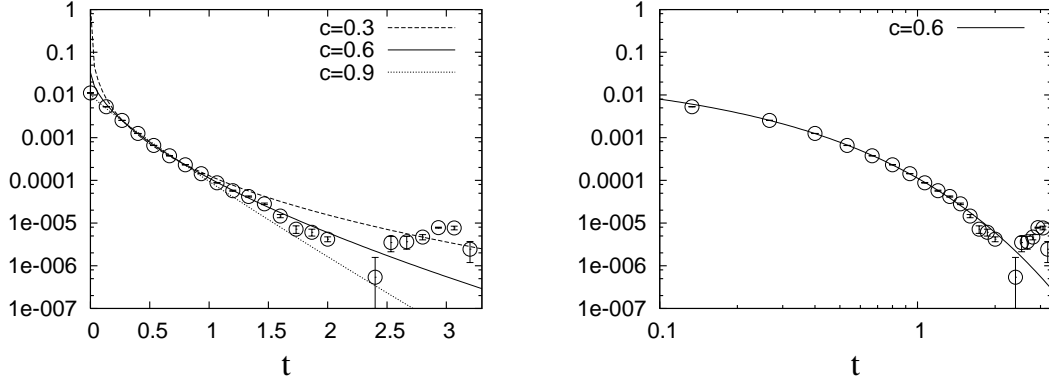


Figure 8: (Left) The two-point correlation function of the non-BPS operator \mathcal{O}_{kl} is plotted for $N = 3$, $1/\beta = 0.15$, $\Lambda = 16$. The curves represent the fits to the form $a \exp(-bt^c)$ with $c = 0.3, 0.6, 0.9$. Fitting the data in the region $0.2 \leq t \leq 1.5$ gives $c = 0.58(2)$. (Right) The log-log plot of the same correlation function, which reveals clear deviation from a straight line behavior corresponding to the power law. The solid line represents a fit to the behavior $a \exp(-bt^c)$ with $c = 0.6$.

with $c = 3/5$. This suggests the existence of a universal mechanism for generating a mass scale in the case of non-supergravity operators.

4. Summary and discussions

In this paper we have studied the strong coupling dynamics of Matrix theory by investigating the IR behavior of two-point correlation functions. As we have reviewed in section 2, various predictions can be obtained from the bulk supergravity analysis based on the gauge-gravity correspondence. The direct calculations on the gauge theory side are completely out of reach of perturbative analyses, however. This motivated us to perform detailed Monte Carlo evaluation of the gauge-theory correlators. Let us briefly summarize the salient features of our results.

- (a) The correlation functions of operators corresponding to the supergravity modes show the power-law behavior with the power consistent with the prediction. Note, in particular, that our Monte Carlo results are obtained at $N = 2$ and 3 , while the supergravity analysis is valid naively at $N = \infty$. Finite N effects, if they exist, would be of the order of $1/N^2$, which is 25% and 11% for $N = 2$ and $N = 3$, respectively. Since the agreement with the supergravity predictions is much more accurate, it is conceivable that the power is actually independent of N (≥ 2).
- (b) The power-law behavior seems to extend beyond the range (1.2) suggested by the validity of the supergravity analysis. Note that our results for $N = 2$ shown in fig. 1 (Left), for instance, include the data around $t \sim 1.5$, while the upper end of the range (1.2) is around $t \sim 1.4$ and 1.7 for $N = 2$ and 3 , respectively. It seems reasonable to consider that the power law would continue to be valid beyond this bound if we increase the IR cutoff β . Indeed, the results in the momentum space shown in fig. 2

suggest that the power law is valid even at $p/(2\pi) \sim 0.2$, which is much smaller than $1/t \sim (1.5)^{-1} \sim 0.72$. This points to the interesting possibility that the power law with the particular power predicted within the range (1.2) is actually valid even in the far IR region $t \sim N \rightarrow \infty$ corresponding to M-theory. We consider it important to explore the implication of this statement on the wave function of the 11-dimensional graviton. In particular, the meaning of the anomalous behavior [14] with respect to the 11D boost transformation discussed in section 2.3 must be clarified.

- (c) As for the stringy excitations, we only have semi-quantitative predictions for the BMN-type operators with large J and large wave number n . Our Monte Carlo results for the BMN-type operators with $J = 2, 3$ provide some evidence that the predicted form $\exp(-bt^{3/5})$ is valid even at small J , although the coefficient b has J -dependence different from what is expected at large J . The same form is also found to fit well our results for other non-BPS operators corresponding to stringy excited modes. Our results therefore suggest that this peculiar behavior may be a universal feature of the mechanism for mass scale generation in Matrix theory.

In order to understand the physical meaning of the observed behaviors of the correlation functions, we have discussed the spectral representation of the correlation functions in appendix A. The power-law behavior for the supergravity modes can be naturally understood as a consequence of the existence of the zero-energy bound state. On the other hand, the exponential behavior $\exp(-bt^{3/5})$ for the stringy excited modes corresponds to a very peculiar form of the spectral function. It would be interesting to clarify possible implications of these properties on M-theory.

Let us list some possible directions for future works. First of all, it is obviously worthwhile to extend the Monte Carlo studies to larger N and larger β , which would further clarify our observations (a) and (b) given above. It would be also important to study various other operators corresponding to stringy excited modes and to test the universal behavior stated in (c). On the technical side, it is important to clarify the issue related to the sign problem in Monte Carlo simulation discussed in appendix C.

From the viewpoint of testing the gauge-gravity correspondence, it is also interesting to pay attention to the normalization, including the sign, of the correlation functions. For instance, the Ward-like identities for correlation functions are discussed [28] using the gauge-gravity correspondence in the non-conformal case including the case of D0-branes. It would be interesting to test such identities by our Monte Carlo method, which would also serve as a self-consistency check of the method itself.

From a more general perspective of the gauge-gravity correspondence, it would be interesting to extend our work to gauge theories in higher dimensions. Of particular interest is to test the AdS-CFT correspondence by studying four-dimensional $\mathcal{N} = 4$ $SU(N)$ SYM by Monte Carlo methods, since most of the tests given so far are not quantitative except for some special cases in which perturbative analyses on the gauge theory side turned out to be useful. In fact, a first step in this direction is taken already. In refs. [37], matrix quantum mechanics of 6 bosonic commuting matrices [38] is shown to give results consistent with

the AdS-CFT correspondence for the three-point functions of chiral primary operators. More recently, Monte Carlo studies of the 4d $\mathcal{N} = 4$ SYM have been performed [39, 40] based on the novel large- N reduction [41], which reduces the calculation in the SYM (in the planar large- N limit) to that in the BMN matrix model [29]. The advantage of this method is that supersymmetry is maximally respected. In particular, there is no need for fine-tuning the parameters in the regularized theory unlike the proposals based on the lattice regularization [42]. See ref. [43] for a proposal to combine a two-dimensional lattice with a fuzzy sphere in order to study the 4d theory at finite N without fine-tuning.

It is also interesting to study the two-dimensional $\mathcal{N} = 8$ $SU(N)$ SYM by Monte Carlo methods. This corresponds to a system of coincident D1-branes, which has an interesting connection [44] to the black hole/black string transition as exhibited by the phase diagram with respect to the temperature and the spatial volume. This system has been studied in the strongly coupled (low temperature) regime by using the dual type II supergravity, and the existence of a first-order transition is conjectured [44]. On the other hand, the weak coupling (high temperature) regime can be described effectively by a bosonic matrix quantum mechanics, in which two phase transitions of second and third orders are found [45, 46]. It is interesting to investigate how the two transitions merge into one as the coupling constant is increased (i.e., as the temperature is decreased) by direct Monte Carlo methods. A lattice simulation of two-dimensional SYM with 4 supercharges and the $SU(2)$ gauge group was started a few years ago [47], and was extended to $SU(N)$ with $N = 2, 3, 4, 5$ [48]. It was shown that fine-tuning of parameters is not necessary in these cases. Recently the 16 supercharge case [49] has been studied. Let us also recall that the (1+1)D SYM with 16 supercharges is termed “Matrix String Theory” as a possible non-perturbative description of type IIA superstring theory in ten dimensions [50]. This theory is closely related with the doubly-compactified supermembranes in 11 dimensions [51], and hence with Matrix theory studied in this paper. It would be very interesting to explore various non-perturbative relations between the two gauge theories by Monte Carlo methods.

To conclude, with the various new ideas on how to treat supersymmetry on a computer, we consider that interesting non-perturbative physics in supersymmetric gauge theories, including those relevant to string theory, has become accessible by Monte Carlo simulation. We hope that our work not only provides further motivation to pursue the Matrix theory conjecture, but also encourages further development in Monte Carlo studies of supersymmetric gauge theories.

Acknowledgments

We thank M. Terashi for his contribution at the early stage of this work. We are also grateful to O. Aharony, Y. Kikukawa and K. Skenderis for useful discussions and comments. Computations have been carried out on PC clusters at KEK and Yukawa Institute. The present work is supported in part by Grant-in-Aid for Scientific Research (No. 20540286 and 23244057 for J.N., No. 21740216 for Y.S. and No. 20340048 for T.Y.) from Japan Society for the Promotion of Science. The work of M. H. is supported from Postdoctoral Fellowship for Research Abroad by Japan Society for the Promotion of Science.

A. Spectral representation of the correlation functions

In this section we discuss the physical meaning of the two-point correlation functions in Matrix theory suggested from the gauge-gravity duality and from direct Monte Carlo calculation. For that purpose we consider the spectral representation

$$\langle O(t) O(0) \rangle = \int_0^\infty d\mu \rho(\mu) \Delta(t, \mu) , \quad (\text{A.1})$$

$$\Delta(t, \mu) = \int \frac{dp}{2\pi} \frac{e^{ipt}}{p^2 + \mu^2} \sim \frac{1}{2\mu} e^{-\mu|t|} \quad (\text{A.2})$$

in the Euclidean space.

Let us first discuss the form (2.16) for the supergravity operators. This corresponds to the spectral representation $\rho(\mu) \sim \mu^{2\nu+1}$. For $2\nu + 1 > 0$, the μ -integral in (A.1) is convergent and one retrieves (2.16). For $2\nu + 1 < 0$, we again invoke analytic continuation in ν . This is in sharp contrast to the free-theory behavior $|t|^n$ ($n = 1, 2, 3, \dots$), which corresponds the spectral functions with delta-function-like singularities at $\mu = 0$. The milder power-law singularity in the spectral function may be regarded as a signature for the existence of a zero-energy bound state as a result of very non-trivial IR dynamics. The fact that ν increases with the angular momentum ℓ is consistent qualitatively with the existence of many-body states which consist of the zero-energy bound states, since the distance scale of such states can grow faster for larger ℓ with a power-law behavior as the energy increases.

Let us next discuss the operators corresponding to stringy excited modes. According to the scaling argument in sections 2.3 and 2.4, the general form of two-point correlators is given by

$$\langle O(t) O(0) \rangle \sim q^{(\Delta+6)/5} \frac{1}{g_s^2 \ell_s^8} |t|^{-(7\Delta+12)/5} f\left(\frac{g_s N |t|^3}{\ell_s^3}\right) . \quad (\text{A.3})$$

For the BMN-type operators with large angular momentum J and a large wave number n , one obtains the prediction for the function $f(g_s N |t|^3 / \ell_s^3)$ at large distances as [16]¹⁷

$$f\left(\frac{g_s N |t|^3}{\ell_s^3}\right) \sim \exp\left(-K \frac{q^{1/5} |t|^{3/5}}{J}\right) \quad (\text{A.4})$$

apart from a possible power-law prefactor, with K being an operator-dependent constant. As the spectral function corresponding to the behavior (A.4), let us consider

$$\rho(\mu) \sim \exp\left(C \mu^{a+1}\right) , \quad (\text{A.5})$$

up to a possible power-law correction factor. At large $|t|$, the μ -integral is dominated by the saddle point $\mu = \left(|t|/(a+1)C\right)^{1/a}$. Comparing the resulting integral with (A.4), we can determine the parameters a and C . Plugging them into (A.5), we get

$$\rho(\mu) \sim \exp\left\{-\frac{2}{3} \left(\frac{3K}{5J}\right)^{5/2} q^{1/2} \mu^{-3/2}\right\} . \quad (\text{A.6})$$

¹⁷The time coordinate used in the first paper of ref. [16] is rescaled from ours by $t \rightarrow q^{1/2}t$.

This is quite different from a simple delta-function $\rho(\mu) \sim \delta(\mu - M)$, which represents the standard asymptotic behavior of the propagator $e^{-M|t|}$ for a massive particle state. At low energy $\mu \rightarrow 0$, the spectral function (A.6) decreases exponentially, which suggests that the *single-body* zero-energy bound state does not directly contribute to the intermediate states. On the other hand, the expression (A.6) approaches a constant if we naively extrapolate it to larger μ . However, it is expected that the power-law prefactor in (A.3) becomes important in this regime. Since the prefactor is essentially the same as in the case of operators corresponding to supergravity modes due to the scaling symmetry, we consider that the *many-body* states consisting of the zero-energy bound state play a dominant role at high energy.

B. The algorithm for Monte Carlo simulation

In this section we explain the details of the algorithm we use for Monte Carlo simulation. In order to treat fermions efficiently, it is crucial to use the idea of the Hybrid Monte Carlo (HMC) algorithm [52].

Let us first discuss the idea for the bosonic part (3.5) neglecting the fermionic part. We introduce the (fictitious) momentum variables

$$\Pi_i^{ab}(t) = \sum_{n=-\Lambda}^{\Lambda} \tilde{\Pi}_{in}^{ab} e^{i\omega n t} , \quad (\text{B.1})$$

which are conjugate to $X_i^{ab}(t)$. Due to the Hermiticity of $\Pi_i^{ab}(t)$, we have the constraint

$$\tilde{\Pi}_{i,-n}^{ab} = (\tilde{\Pi}_{in}^{ba})^* . \quad (\text{B.2})$$

Similarly, we introduce the momentum variables p_a corresponding to α_a . Then we define the fictitious Hamiltonian for the bosonic part as

$$H_b = \frac{1}{2} \sum_{a=1}^N (p_a)^2 + \frac{1}{2} \sum_{n=-\Lambda}^{\Lambda} \tilde{\Pi}_{in}^{ab} \tilde{\Pi}_{i,-n}^{ba} + S_b[X, \alpha] . \quad (\text{B.3})$$

The Hamilton equation can be obtained as

$$\frac{d\tilde{X}_{in}^{ab}}{d\tau} = \frac{\partial H_b}{\partial \tilde{\Pi}_{in}^{ab}} = \tilde{\Pi}_{i,-n}^{ba} \quad (\text{B.4})$$

$$\frac{d\tilde{\Pi}_{in}^{ab}}{d\tau} = -\frac{\partial H_b}{\partial \tilde{X}_{in}^{ab}} = -\frac{\partial S_b[X, \alpha]}{\partial \tilde{X}_{in}^{ab}} . \quad (\text{B.5})$$

By using the explicit form of $S_b[X, \alpha]$, we can calculate the second line explicitly as

$$\begin{aligned} \frac{d\tilde{\Pi}_{in}^{ab}}{d\tau} = & -N\beta \left[\left(n\omega - \frac{1}{\beta}(\alpha_a - \alpha_b) \right)^2 \tilde{X}_{i,-n}^{ba} \right. \\ & \left. + 2(\tilde{X}_i \tilde{X}_j \tilde{X}_j)_{-n}^{ba} - 4(\tilde{X}_j \tilde{X}_i \tilde{X}_j)_{-n}^{ba} + 2(\tilde{X}_j \tilde{X}_j \tilde{X}_i)_{-n}^{ba} \right] . \end{aligned} \quad (\text{B.6})$$

Similarly, the Hamilton equations for the gauge variables are obtained as

$$\frac{d\alpha_a}{d\tau} = \frac{\partial H_b}{\partial p_a} = p_a \quad (\text{B.7})$$

$$\frac{dp_a}{d\tau} = -\frac{\partial H_b}{\partial \alpha_a} = 2N \sum_{n=-\Lambda}^{\Lambda} \left(n\omega - \frac{1}{\beta}(\alpha_a - \alpha_b) \right) \tilde{X}_{in}^{ab} \tilde{X}_{i,-n}^{ba} . \quad (\text{B.8})$$

Updating the bosonic variables is performed by (i) refreshing the momentum variables p_a and $\tilde{\Pi}_{in}^{ab}$ by Gaussian random numbers, which obey the distribution e^{-H_b} and (ii) solving the Hamilton equations for a fixed time interval τ . In order to satisfy the detailed balance, one needs to adopt the so-called leap-frog discretization for τ -evolution, and to perform the Metropolis accept/reject procedure after (ii) with the acceptance probability $\min(1, e^{-\Delta H_b})$. For more details, see refs. [53, 54], in which the method is described for supersymmetric matrix models.

Let us next introduce fermions. We expand the Fourier component $\tilde{\psi}_{\alpha n}$ of the fermion field as

$$\tilde{\psi}_{\alpha n} = \sum_{A=1}^{N^2} \tilde{\psi}_{\alpha n}^A t^A \quad (\text{B.9})$$

in terms of $U(N)$ generators t^A . (We will impose the traceless condition later.) Here we use a representation given by

$$(t^A)_{ab} = \delta_{ai_A} \delta_{bj_A} , \quad (\text{B.10})$$

where $a = 1, \dots, N^2$, and we have defined

$$A = N(i_A - 1) + j_A , \quad (\text{B.11})$$

$$\bar{A} = N(j_A - 1) + i_A , \quad (\text{B.12})$$

with which we may write

$$\text{Tr}(t^A t^B) = \delta_{\bar{A}B} . \quad (\text{B.13})$$

Let us also define

$$g_{ABC} \equiv \text{Tr} \left(t^C [t^A, t^B] \right) = \delta_{j_A i_B} \delta_{j_B i_C} \delta_{j_C i_A} - \delta_{j_C i_B} \delta_{j_B i_A} \delta_{j_A i_C} . \quad (\text{B.14})$$

Then the fermionic action S_f given in eq. (3.6) may be written in the form

$$S_f = \frac{1}{2} \mathcal{M}'_{A\alpha n; B\beta p} \tilde{\psi}_{\alpha n}^A \tilde{\psi}_{\beta p}^B , \quad (\text{B.15})$$

where we have defined a matrix \mathcal{M}' of dimension $16(2\Lambda + 1)N^2$ by

$$\mathcal{M}'_{A\alpha p, B\beta q} = -\beta (\gamma_i)^{\alpha\beta} \tilde{X}_{ip-q}^C g_{ABC} + \beta \delta_{pq} \left(i p \omega - i \frac{1}{\beta} (\alpha_{i_B} - \alpha_{j_B}) \right) \delta_{\alpha\beta} \delta_{\bar{A}B} . \quad (\text{B.16})$$

We impose the traceless condition on the fermion field by making the replacement

$$(\tilde{\psi}_{\alpha n})^{NN} \mapsto - \sum_{a=1}^{N-1} (\tilde{\psi}_{\alpha n})^{aa} . \quad (\text{B.17})$$

The fermion action can be written in terms of the remaining degrees of freedom as

$$\tilde{\psi}_{\alpha p}^A \mathcal{M}'_{A\alpha p, B\beta q} \tilde{\psi}_{\beta q}^B = \tilde{\psi}_{\alpha p}^{A'} \mathcal{M}_{A'\alpha p, B'\beta q} \tilde{\psi}_{\beta q}^{B'} , \quad (\text{B.18})$$

where we have defined a matrix \mathcal{M} of dimension $16(2\Lambda + 1)(N^2 - 1)$ by

$$\begin{aligned} \mathcal{M}_{A'\alpha p, B'\beta q} &= \mathcal{M}'_{A'\alpha p, B'\beta q} - \mathcal{M}'_{N^2\alpha p, B\beta q} \delta_{i_{A'} j_{A'}} \\ &\quad - \mathcal{M}'_{A'\alpha p, N^2\beta q} \delta_{i_{B'} j_{B'}} + \mathcal{M}'_{N^2\alpha p, N^2\beta q} \delta_{i_{A'} j_{A'}} \delta_{i_{B'} j_{B'}} . \end{aligned} \quad (\text{B.19})$$

Integrating out the fermions, we obtain $\text{Pf}\mathcal{M}$, which is complex in general. As we explained below (3.6), we simply replace it by its absolute value

$$|\text{Pf}\mathcal{M}| = \det(\mathcal{D}^{1/4}) , \quad (\text{B.20})$$

where $\mathcal{D} = \mathcal{M}^\dagger \mathcal{M}$.

The trick of the RHMC algorithm [36] is to represent $|\text{Pf}\mathcal{M}|$ as

$$|\text{Pf}\mathcal{M}| = \int dF dF^* e^{-S_{\text{PF}}} , \quad (\text{B.21})$$

where

$$S_{\text{PF}} = a_0 F^* F + \sum_{k=1}^Q a_k F^* (\mathcal{D} + b_k)^{-1} F , \quad (\text{B.22})$$

using the auxiliary complex variables F , which are called pseudo-fermions. Here the constants a_k and b_k are real positive parameters appearing in the rational approximation

$$x^{-1/4} \simeq a_0 + \sum_{k=1}^Q \frac{a_k}{x + b_k} , \quad (\text{B.23})$$

and they can be generated by a code [55] based on the Remez algorithm. The approximation (B.23) can be made to have sufficiently small relative errors (smaller than δ) within a certain range ($\epsilon < x < 1$). In our simulation, we use $Q = 15$ with $\delta = 1.19 \times 10^{-4}$ and $\epsilon = 10^{-12}$. We rescale the matrix \mathcal{D} by an appropriate constant factor so that the largest eigenvalue of \mathcal{D} is well below the upper bound for the approximation.

Then we apply the usual HMC algorithm to the whole system. The Hamiltonian for the pseudo-fermions is given by

$$H_{\text{PF}} = \sum_I \Phi_I^* \Phi_I + S_{\text{PF}} , \quad (\text{B.24})$$

where the field Φ represents the momentum variables conjugate to the pseudo-fermions F . Here and henceforth, the index I is used to represent the spinor index α , the momentum index n and the $\text{SU}(N)$ index A , collectively. The Hamilton equations for the pseudo-fermions are given by

$$\frac{dF_I}{d\tau} = \frac{\partial H_{\text{PF}}}{\partial \Phi_I} = \Phi_I^* \quad (\text{B.25})$$

$$\frac{d\Phi_I}{d\tau} = -\frac{\partial H_{\text{PF}}}{\partial F_I} = -a_0 F_I^* - \sum_{k=1}^Q a_k G_I^{(k)*} , \quad (\text{B.26})$$

where $G_I^{(k)}$ is defined by

$$\left(\mathcal{M}^\dagger \mathcal{M} + b_k\right)_{IJ} G_J^{(k)} = F_I \quad \text{for } k = 1, \dots, Q. \quad (\text{B.27})$$

We have to add extra terms

$$-\frac{\partial S_{\text{PF}}}{\partial \tilde{X}_{in}^{ab}} = \sum_{k=1}^Q a_k G^{(k)*} \left(\mathcal{M}^\dagger \frac{\partial \mathcal{M}}{\partial \tilde{X}_{in}^{ab}} + \frac{\partial \mathcal{M}^\dagger}{\partial \tilde{X}_{in}^{ab}} \mathcal{M} \right) G^{(k)}, \quad (\text{B.28})$$

$$-\frac{\partial S_{\text{PF}}}{\partial \alpha_a} = \sum_{k=1}^Q a_k G^{(k)*} \left(\mathcal{M}^\dagger \frac{\partial \mathcal{M}}{\partial \alpha_a} + \frac{\partial \mathcal{M}^\dagger}{\partial \alpha_a} \mathcal{M} \right) G^{(k)} \quad (\text{B.29})$$

on the right-hand side of eqs. (B.5) and (B.8), respectively.

The main part of the computation comes from solving a linear system (B.27). We solve the system for the smallest b_k using the conjugate gradient method, which reduces the problem to the iterative multiplications of \mathcal{M} to a pseudo-fermion field, each of which requires $\mathcal{O}(\Lambda^2 N^3)$ arithmetic operations.¹⁸ The solutions for larger b_k 's can be obtained as by-products using the idea of the multi-mass Krylov solver [56]. This avoids the factor of Q increase of the computational effort.

When we solve the fictitious classical Hamilton dynamics, the step size of the discretized evolution may depend on the Fourier mode. We take the step size to be proportional to the average fluctuation of each mode of the bosonic matrices so that the configuration space can be swept out most efficiently. This technique is called the Fourier acceleration [35]. In the lattice gauge theory, in order to apply the Fourier acceleration one has to transform the configuration to the momentum representation. On the other hand, in the present momentum cutoff method, the Fourier acceleration can be implemented without any additional cost since we are working directly in the momentum space. Thanks to this advantage, the efficiency of the algorithm is enhanced drastically.

In actual simulation, we observe certain instability [18], which is related to the existence of the flat direction $[X_i, X_j] \approx 0$ in the potential term of the action (3.1). This instability can be seen by probing the observable

$$R^2 \equiv \frac{1}{N\beta} \int_0^\beta dt \text{Tr} (X_i)^2. \quad (\text{B.30})$$

Typically this quantity fluctuates around some value, but sometimes it grows rapidly and the simulation bumps. In order to avoid this problem, we introduce a cutoff on R^2 , which is taken to be sufficiently larger than the upper edge of the fluctuation. The value of the cutoff is 5.0 and 3.8 for $N = 2$ and $N = 3$, respectively.

C. Sign problem

In this section we discuss the so-called sign problem in Monte Carlo studies of Matrix theory (3.1). As we explained below eq. (3.6), we neglect the phase of the Pfaffian that appears from integrating out fermionic matrices.

¹⁸Note that one should not construct \mathcal{M} explicitly and multiply it to a pseudo-fermion field literally, which would require $\mathcal{O}(\Lambda^2 N^4)$ arithmetic operations. Instead one should reduce the procedure to multiplication of $N \times N$ matrices using the original definition of \mathcal{M} .

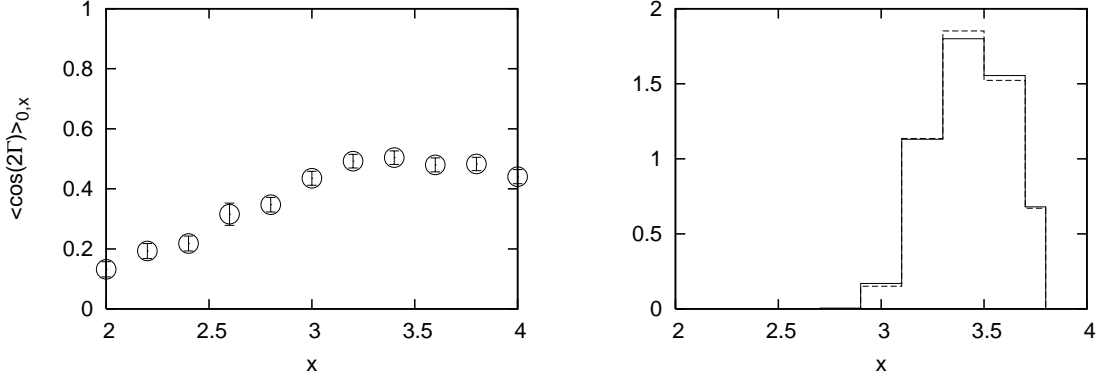


Figure 9: (Left) The VEV $\langle \cos 2\Gamma \rangle_{0,x}$ is plotted for SU(3), $\beta = 6.67$, $\Lambda = 8$. (Right) The distribution $\rho^{(0)}(x)$ and the product $\tilde{\rho}(x) \propto \rho^{(0)}(x)\tilde{w}(x)$ with the normalization $\int dx \tilde{\rho}(x) = 1$ are plotted by the solid line and the dashed line, respectively. SU(3), $\beta = 6.67$, $\Lambda = 8$.

Here we present some numerical evidence, which shows that the effect of the phase is indeed small. As a typical observable, let us consider R^2 defined by (B.30), and discuss how it is affected by the fluctuation of the phase. For that purpose we use the factorization method [57, 58, 59], which was proposed to study the effect of the phase in a general model suffering from the sign problem. Let us define the distribution function

$$\rho(x) = \left\langle \delta(x - R^2) \right\rangle, \quad (\text{C.1})$$

$$\rho^{(0)}(x) = \left\langle \delta(x - R^2) \right\rangle_0, \quad (\text{C.2})$$

for the full model and for the phase-quenched model, respectively. One can then easily show that

$$\rho(x) \propto \rho^{(0)}(x) w(x), \quad (\text{C.3})$$

where the correction factor $w(x)$ is given by

$$w(x) \equiv \left\langle e^{i\Gamma} \right\rangle_{0,x} = \left\langle \cos \Gamma \right\rangle_{0,x}. \quad (\text{C.4})$$

Here, Γ represents the phase of the Pfaffian, and the symbol $\langle \cdot \rangle_{0,x}$ represents a VEV with respect to the phase-quenched model with the constraint $R^2 = x$.

Since the calculation of $\text{Pf}\mathcal{M}$ is time-consuming, we calculate $\det\mathcal{M} = (\text{Pf}\mathcal{M})^2$, from which we can obtain $\tilde{w}(x) \equiv \left\langle \cos(2\Gamma) \right\rangle_{0,x}$. This is sufficient for estimating an upper bound on the effect of the phase since the factor of 2 in the cosine only magnifies it. In fig. 9 (Left) we plot $\tilde{w}(x)$ for $N = 3$, $\beta = 6.67$ and $\Lambda = 8$. In fig. 9 (Right) we plot the distribution function $\rho^{(0)}(x)$ for the phase-quenched model and the product $\tilde{\rho}(x) \propto \rho^{(0)}(x)\tilde{w}(x)$ with the normalization $\int dx \tilde{\rho}(x) = 1$. The difference between $\tilde{\rho}(x)$ and $\rho^{(0)}(x)$ is indeed negligible, which implies that the expectation value $\langle R^2 \rangle$ is not affected by the effect of the phase.

We speculate that the phase quenching can be completely justified in the large- β limit. At large β , the expectation value of $\langle R^2 \rangle$ can be obtained by solving the saddle-point

equation

$$\frac{d}{dx} \ln \rho^{(0)}(x) = -\frac{d}{dx} \ln w(x) . \quad (\text{C.5})$$

First, we can easily prove that the Pfaffian becomes real if we omit the kinetic term in (3.6). As β increases, there are actually more and more low-momentum modes, for which the kinetic term is small. Therefore, we consider it conceivable that the fluctuation of the phase does not increase as $O(\sqrt{\beta})$, which is the typical growth of the fluctuation for extensive quantities at large β . As a result, the right-hand side of (C.5) is expected to be $O(\beta^p)$ with $p < 1$, whereas the left-hand side is expected to be $O(\beta)$ according to the usual scaling argument. In fig. 9 we do observe that the x dependence of $\tilde{w}(x)$ is much smaller than that of $\rho^{(0)}(x)$. If our scenario is correct, we can neglect the effect of the phase completely in the $\beta \rightarrow \infty$ limit. In order to confirm this scenario, we need to investigate the β dependence, which we leave for future investigations.

References

- [1] T. Banks, W. Fischler, S. H. Shenker and L. Susskind, *M theory as a matrix model: A conjecture*, *Phys. Rev. D* **55** (1997) 5112 [[hep-th/9610043](#)].
For a comprehensive review of Matrix theory, see, *e.g.*, W. Taylor, *M(atrix) theory: Matrix quantum mechanics as a fundamental theory*, *Rev. Mod. Phys.* **73** (2001) 419 [[hep-th/0101126](#)].
- [2] E. Witten, *String theory dynamics in various dimensions* *Nucl. Phys. B* **443** (1995) 85 [[hep-th/9503124](#)].
- [3] C. M. Hull and P. K. Townsend, *Unity of superstring dualities* *Nucl. Phys. B* **438** (1995) 109 [[hep-th/9410167](#)].
- [4] E. Witten, *Bound states of strings and p-branes* *Nucl. Phys. B* **460** (1996) 335 [[hep-th/9510135](#)].
- [5] B. de Wit, J. Hoppe and H. Nicolai, *On the quantum mechanics of supermembranes*, *Nucl. Phys. B* **305** (1988) 545.
- [6] Y. Okawa and T. Yoneya, *Multi-body interactions of D-particles in supergravity and matrix theory*, *Nucl. Phys. B* **538** (1999) 67 [[hep-th/9806108](#)]; *Equations of motion and Galilei invariance in D-particle dynamics*, *Nucl. Phys. B* **541** (1999) 163 [[hep-th/9808188](#)].
- [7] J. M. Maldacena, *The large N limit of superconformal field theories and supergravity*, *Adv. Theor. Math. Phys.* **2** (1998) 231 [*Int. J. Theor. Phys.* **38** (1999) 1113, [hep-th/9711200](#)].
- [8] N. Itzhaki, J. M. Maldacena, J. Sonnenschein and S. Yankielowicz, *Supergravity and the large N limit of theories with sixteen supercharges*, *Phys. Rev. D* **58** (1998) 046004 [[hep-th/9802042](#)].
- [9] A. Jevicki and T. Yoneya, *Space-time uncertainty principle and conformal symmetry in D-particle dynamics*, *Nucl. Phys. B* **535** (1998) 335 [[hep-th/9805069](#)].
- [10] A. Jevicki, Y. Kazama and T. Yoneya, *Generalized conformal symmetry in D-brane matrix models*, *Phys. Rev. D* **59** (1999) 066001 [[hep-th/9810146](#)].

- [11] Y. Sekino and T. Yoneya, *Generalized AdS-CFT correspondence for matrix theory in the large N limit*, *Nucl. Phys.* **B 570** (2000) 174 [[hep-th/9907029](#)];
Y. Sekino, *Supercurrents in matrix theory and the generalized AdS/CFT correspondence*, *Nucl. Phys.* **B 602** (2001) 147 [[hep-th/0011122](#)].
- [12] S. S. Gubser, I. R. Klebanov and A. M. Polyakov, *Gauge theory correlators from non-critical string theory*, *Phys. Lett.* **B 428** (1998) 105 [[hep-th/9802109](#)];
E. Witten, *Anti-de Sitter space and holography*, *Adv. Theor. Math. Phys.* **2** (1998) 253 [[hep-th/9802150](#)].
- [13] D. N. Kabat and W. Taylor, *Linearized supergravity from matrix theory*, *Phys. Lett.* **B 426** (1998) 297 [[hep-th/9712185](#)];
W. Taylor and M. Van Raamsdonk, *Supergravity currents and linearized interactions for matrix theory configurations with fermionic backgrounds*, *JHEP* **04** (1999) 013 [[hep-th/9812239](#)]; *Multiple D0-branes in weakly curved backgrounds*, *Nucl. Phys.* **B 558** (1999) 63 [[hep-th/9904095](#)].
- [14] T. Yoneya, *Generalized conformal symmetry and oblique AdS/CFT correspondence for matrix theory*, *Class. Quant. Grav.* **17** (2000) 1307 [[hep-th/9908153](#)].
- [15] P. Yi, *Witten index and threshold bound states of D-branes*, *Nucl. Phys.* **B 505** (1997) 307 [[hep-th/9704098](#)];
S. Sethi and M. Stern, *D-brane bound states redux*, *Commun. Math. Phys.* **194** (1998) 675 [[hep-th/9705046](#)];
G. W. Moore, N. Nekrasov and S. Shatashvili, *D-particle bound states and generalized instantons*, *Commun. Math. Phys.* **209** (2000) 77 [[hep-th/9803265](#)].
- [16] M. Asano, Y. Sekino and T. Yoneya, *PP-wave holography for Dp-brane backgrounds*, *Nucl. Phys.* **B 678** (2004) 197 [[hep-th/0308024](#)].
M. Asano and Y. Sekino, *Large N limit of SYM theories with 16 supercharges from superstrings on Dp-brane backgrounds*, *Nucl. Phys.* **B 705** (2005) 33 [[hep-th/0405203](#)].
M. Asano, *Stringy effect of the holographic correspondence for Dp-brane backgrounds*, *JHEP* **12** (2004) 029 [[hep-th/0408030](#)].
- [17] M. Hanada, J. Nishimura and S. Takeuchi, *Non-lattice simulation for supersymmetric gauge theories in one dimension*, *Phys. Rev. Lett.* **99** (2007) 161602 [[arXiv:0706.1647](#)].
- [18] K. N. Anagnostopoulos, M. Hanada, J. Nishimura and S. Takeuchi, *Monte Carlo studies of supersymmetric matrix quantum mechanics with sixteen supercharges at finite temperature*, *Phys. Rev. Lett.* **100** (2008) 021601 [[arXiv:0707.4454](#)].
- [19] M. Hanada, Y. Hyakutake, J. Nishimura and S. Takeuchi, *Higher derivative corrections to black hole thermodynamics from supersymmetric matrix quantum mechanics*, *Phys. Rev. Lett.* **102** (2009) 191602 [[arXiv:0811.3102](#)].
- [20] M. Hanada, A. Miwa, J. Nishimura and S. Takeuchi, *Schwarzschild radius from Monte Carlo calculation of the Wilson loop in supersymmetric matrix quantum mechanics*, *Phys. Rev. Lett.* **102** (2009) 181602 [[arXiv:0811.2081](#)].
- [21] A. V. Smilga, *Comments on thermodynamics of supersymmetric matrix models*, *Nucl. Phys.* **B 818** (2009) 101 [[arXiv:0812.4753](#)].
- [22] M. Hanada, S. Matsuura, J. Nishimura and D. Robles-Llana, *Nonperturbative studies of supersymmetric matrix quantum mechanics with 4 and 8 supercharges at finite temperature*, *JHEP* **02** (2011) 060 [[arXiv:1012.2913](#)].

- [23] J. R. Hiller, S. S. Pinsky, N. Salwen and U. Trittman, *Direct evidence for the Maldacena conjecture for $\mathcal{N} = (8,8)$ super Yang-Mills theory in 1+1 dimensions*, *Phys. Lett. B* **624** (2005) 105 [[hep-th/0506225](#)].
- [24] M. Hanada, J. Nishimura, Y. Sekino and T. Yoneya, *Monte Carlo studies of Matrix theory correlation functions*, *Phys. Rev. Lett.* **104** (2010) 151601 [[arXiv:0911.1623](#)].
- [25] T. Yoneya, *String theory and space-time uncertainty principle*, *Prog. Theor. Phys.* **103** (2000) 1081 [[hep-th/0004074](#)].
- [26] G. T. Horowitz and A. Strominger, *Black strings and P-branes*, *Nucl. Phys. B* **360** (1991) 197.
See also, G. W. Gibbons and K. Maeda, *Black holes and membranes in higher dimensional theories with dilaton fields*, *Nucl. Phys. B* **298** (1988) 741.
- [27] T. Azeanagi, M. Hanada, H. Kawai and Y. Matsuo, *Worldsheet analysis of gauge/gravity dualities*, *Nucl. Phys. B* **816** (2009) 278 [[arXiv:0812.1453](#)].
- [28] I. Kanitscheider, K. Skenderis and M. Taylor, *Precision holography for non-conformal branes*, *JHEP* **09** (2008) 094 [[arXiv:0807.3324](#)].
- [29] D. E. Berenstein, J. M. Maldacena and H. S. Nastase, *Strings in flat space and pp waves from $\mathcal{N} = 4$ super Yang Mills*, *JHEP* **04** (2002) 013 [[hep-th/0202021](#)].
- [30] S. Dobashi, H. Shimada and T. Yoneya, *Holographic reformulation of string theory on $AdS_5 \times S^5$ background in the PP-wave limit*, *Nucl. Phys. B* **665** (2003) 94 [[hep-th/0209251](#)].
- [31] T. Yoneya, *Holography in the large J limit of AdS/CFT correspondence and its applications*, *Prog. Theor. Phys. Suppl.* **164** (2007) 82 [[hep-th/0607046](#)].
- [32] S. Dobashi and T. Yoneya, *Resolving the holography in the plane-wave limit of AdS/CFT correspondence*, *Nucl. Phys. B* **711** (2005) 3 [[hep-th/0406225](#)].
- [33] A. Miwa and T. Yoneya, *Holography of Wilson-loop expectation values with local operator insertions*, *JHEP* **12** (2006) 060 [[hep-th/0609007](#)].
A. Tsuji, *Holography of Wilson loop correlator and spinning strings*, *Prog. Theor. Phys.* **117** (2007) 557 [[hep-th/0606030](#)].
- [34] S. Catterall and T. Wiseman, *Towards lattice simulation of the gauge theory duals to black holes and hot strings*, *JHEP* **12** (2007) 104 [[arXiv:0706.3518](#)];
Black hole thermodynamics from simulations of lattice Yang-Mills theory, *Phys. Rev. D* **78** (2008) 041502 [[arXiv:0803.4273](#)];
Extracting black hole physics from the lattice, *JHEP* **04** (2010) 077 [[arXiv:0909.4947](#)].
- [35] S. Catterall and S. Karamov, *Testing a Fourier accelerated hybrid Monte Carlo algorithm*, *Phys. Lett. B* **528** (2002) 301 [[hep-lat/0112025](#)].
- [36] M. A. Clark and A. D. Kennedy, *The RHMC algorithm for 2 flavors of dynamical staggered fermions*, *Nucl. Phys. Proc. Suppl.* **129** (2004) 850 [[hep-lat/0309084](#)].
- [37] D. Berenstein and R. Cotta, *A Monte-Carlo study of the AdS/CFT correspondence: An exploration of quantum gravity effects*, *JHEP* **04** (2007) 071 [[hep-th/0702090](#)];
D. Berenstein, R. Cotta and R. Leonardi, *Numerical tests of AdS/CFT at strong coupling*, *Phys. Rev. D* **78** (2008) 025008. [[arXiv:0801.2739](#)].
- [38] D. Berenstein, *Large N BPS states and emergent quantum gravity*, *JHEP* **01** (2006) 125 [[hep-th/0507203](#)].

- [39] J. Nishimura, *Non-lattice simulation of supersymmetric gauge theories as a probe to quantum black holes and strings*, PoS **LAT2009** (2009) 016 [[arXiv:0912.0327](#)].
- [40] M. Honda, G. Ishiki, S. W. Kim, J. Nishimura and A. Tsuchiya, *Supersymmetry non-renormalization theorem from a computer and the AdS/CFT correspondence*, PoS **LATTICE2010** (2010) 253 [[arXiv:1011.3904](#)].
- [41] T. Ishii, G. Ishiki, S. Shimasaki and A. Tsuchiya, $\mathcal{N}=4$ super Yang-Mills from the plane wave matrix model, *Phys. Rev. D* **78** (2008) 106001 [[arXiv:0807.2352](#)].
G. Ishiki, S. W. Kim, J. Nishimura and A. Tsuchiya, *Deconfinement phase transition in $\mathcal{N}=4$ super Yang-Mills theory on $R \times S^3$ from supersymmetric matrix quantum mechanics*, *Phys. Rev. Lett.* **102** (2009) 111601 [[arXiv:0810.2884](#)].
G. Ishiki, S. W. Kim, J. Nishimura and A. Tsuchiya, *Testing a novel large- N reduction for $\mathcal{N}=4$ super Yang-Mills theory on $R \times S^3$* , *JHEP* **09** (2009) 029 [[arXiv:0907.1488](#)].
- [42] D. B. Kaplan and M. Unsal, *A Euclidean lattice construction of supersymmetric Yang-Mills theories with sixteen supercharges*, *JHEP* **09** (2005) 042 [[hep-lat/0503039](#)].
M. Unsal, *Supersymmetric deformations of type IIB matrix model as matrix regularization of $\mathcal{N}=4$ SYM*, *JHEP* **04** (2006) 002 [[hep-th/0510004](#)].
J. W. Elliott, J. Giedt and G. D. Moore, *Lattice four-dimensional $\mathcal{N}=4$ SYM is practical*, *Phys. Rev. D* **78** (2008) 081701 [[arXiv:0806.0013](#)].
S. Catterall, *First results from simulations of supersymmetric lattices*, *JHEP* **01** (2009) 040 [[arXiv:0811.1203](#)].
J. Giedt, *Progress in four-dimensional lattice supersymmetry*, *Int. J. Mod. Phys. A* **24** (2009) 4045 [[arXiv:0903.2443](#)].
S. Catterall, E. Dzienkowski, J. Giedt, A. Joseph and R. Wells, *Perturbative renormalization of lattice $\mathcal{N}=4$ super Yang-Mills theory*, *JHEP* **04** (2011) 074 [[arXiv:1102.1725](#)].
- [43] M. Hanada, S. Matsuura and F. Sugino, *Two-dimensional lattice for four-dimensional $\mathcal{N}=4$ supersymmetric Yang-Mills*, [arXiv:1004.5513](#).
M. Hanada, *A proposal of a fine tuning free formulation of 4d $\mathcal{N}=4$ super Yang-Mills*, *JHEP* **11** (2010) 112 [[arXiv:1009.0901](#)].
- [44] O. Aharony, J. Marsano, S. Minwalla and T. Wiseman, *Black hole-black string phase transitions in thermal 1+1-dimensional supersymmetric Yang-Mills theory on a circle*, *Class. Quant. Grav.* **21** (2004) 5169 [[hep-th/0406210](#)].
- [45] N. Kawahara, J. Nishimura and S. Takeuchi, *Phase structure of matrix quantum mechanics at finite temperature*, *JHEP* **10** (2007) 097 [[arXiv:0706.3517](#)].
- [46] G. Mandal, M. Mahato and T. Morita, *Phases of one dimensional large N gauge theory in a $1/D$ expansion*, *JHEP* **02** (2010) 034 [[arXiv:0910.4526](#)].
- [47] I. Kanamori, H. Suzuki and F. Sugino, *Euclidean lattice simulation for the dynamical supersymmetry breaking*, *Phys. Rev. D* **77** (2008) 091502 [[arXiv:0711.2099](#)];
Observing dynamical supersymmetry breaking with euclidean lattice simulations, *Prog. Theor. Phys.* **119** (2008) 797 [[arXiv:0711.2132](#)].
I. Kanamori and H. Suzuki, *Restoration of supersymmetry on the lattice: Two-dimensional $\mathcal{N}=(2,2)$ supersymmetric Yang-Mills theory*, *Nucl. Phys. B* **811** (2009) 420 [[arXiv:0809.2856](#)];
Some physics of the two-dimensional $\mathcal{N}=(2,2)$ supersymmetric Yang-Mills theory: Lattice Monte Carlo study, *Phys. Lett. B* **672** (2009) 307 [[arXiv:0811.2851](#)].

- [48] M. Hanada and I. Kanamori, *Lattice study of two-dimensional $\mathcal{N}=(2,2)$ super Yang-Mills at large- N* , *Phys. Rev. D* **80** (2009) 065014 [[arXiv:0907.4966](#)];
Absence of sign problem in two-dimensional $\mathcal{N}=(2,2)$ super Yang-Mills on lattice, *JHEP* **01** (2011) 058 [[arXiv:1010.2948](#)]
- [49] S. Catterall, A. Joseph and T. Wiseman, *Thermal phases of D1-branes on a circle from lattice super Yang-Mills*, *JHEP* **12** (2010) 022 [[arXiv:1008.4964](#)].
- [50] R. Dijkgraaf, E. P. Verlinde and H. L. Verlinde, *Matrix string theory*, *Nucl. Phys. B* **500** (1997) 43 [[arXiv:hep-th/9703030](#)].
- [51] Y. Sekino and T. Yoneya, *From supermembrane to matrix string*, *Nucl. Phys. B* **619** (2001) 22 [[hep-th/0108176](#)].
- [52] S. Duane, A. D. Kennedy, B. J. Pendleton and D. Roweth, *Hybrid Monte Carlo*, *Phys. Lett. B* **195** (1987) 216.
- [53] J. Ambjorn, K. N. Anagnostopoulos, W. Bietenholz, T. Hotta and J. Nishimura, *Large N dynamics of dimensionally reduced 4-D $SU(N)$ superYang-Mills theory*, *JHEP* **07** (2000) 013 [[arXiv:hep-th/0003208](#)].
- [54] J. Ambjorn, K. N. Anagnostopoulos, W. Bietenholz, T. Hotta and J. Nishimura, *Monte Carlo studies of the IIB matrix model at large N* , *JHEP* **07** (2000) 011 [[arXiv:hep-th/0005147](#)].
- [55] M.A. Clark and A.D. Kennedy, <http://www.ph.ed.ac.uk/~mike/remez>, 2005.
- [56] B. Jegerlehner, *Krylov space solvers for shifted linear systems*, [hep-lat/9612014](#).
- [57] K. N. Anagnostopoulos and J. Nishimura, *New approach to the complex action problem and its application to a nonperturbative study of superstring theory*, *Phys. Rev. D* **66** (2002) 106008 [[hep-th/0108041](#)].
- [58] J. Ambjorn, K. N. Anagnostopoulos, J. Nishimura and J. J. M. Verbaarschot, *The factorization method for systems with a complex action: A test in random matrix theory for finite density QCD*, *JHEP* **10** (2002) 062 [[hep-lat/0208025](#)].
- [59] K. N. Anagnostopoulos, T. Azuma and J. Nishimura, *A general approach to the sign problem: The factorization method with multiple observables*, *Phys. Rev. D* **83** (2011) 054504 [[arXiv:1009.4504](#)]; *A practical solution to the sign problem in a matrix model for dynamical compactification*, [arXiv:1108.1534](#).